



Moth Swarm Algorithm for Image Contrast Enhancement

Alberto Luque-Chang ^{a,*}, Erik Cuevas ^a, Marco Pérez-Cisneros ^a, Fernando Fausto ^a, Arturo Valdivia-González ^a, Ram Sarkar ^b

^a Departamento de Electrónica, Universidad de Guadalajara, CUCET Av. Revolución 1500, 44430, Guadalajara, Mexico

^b Department of Computer Science and Engineering, Jadavpur University, Kolkata, 700032, India



ARTICLE INFO

Article history:

Received 24 June 2020

Received in revised form 12 October 2020

Accepted 8 November 2020

Available online 26 November 2020

Keywords:

Image enhancement

Moth Swarm Algorithm

Global optimization

ABSTRACT

Image Contrast Enhancement (ICE) is a crucial step in several image processing and computer vision applications. Its main objective is to improve the quality of the visual information contained in the processed images. The presence of noise and small sets of pixels in images are not only irrelevant for their visualization. It also negatively affects the improvement process of ICE schemes since the inclusion of irrelevant information avoids the appropriate distribution of significant pixel intensities in the enhanced image. As a consequence of this effect, most of the proposed ICE methods present different associated problems such as the production of undesirable artifacts, noise amplification, over saturation and bad human visual perception. In this paper, an Image Contrast Enhancement (ICE) method for grayscale and color images is presented. The proposed approach has the property of eliminating noisy and irrelevant information in order to improve the distribution capacity of significant pixel intensities in the enhanced image. Our method eliminates multiple groups of a very small number of pixels that, according to their characteristics, do not represent any object or important detail of the image. This process is done by the Mean-shift algorithm, which is used to replace such sets of irrelevant pixels in the original histogram by significant pixel densities represented by local maxima. Then, the Moth Swarm Algorithm (MSA) is used to redistribute the pixel intensities of the reduced histogram so that the value from Kullback–Leibler entropy (KL-entropy) has been maximized. The proposed approach has been tested considering different public datasets commonly used in the literature. Its results are also compared with those produced by other well-known ICE techniques. Evaluation of the experimental results demonstrates that the proposed approach highlights the important details of the image also improving its human visual appearance.

© 2020 Elsevier B.V. All rights reserved.

1. Introduction

A Knowledge-Based Systems (KBS) [1] is an area of artificial intelligence that refers to the extraction and representation of the knowledge in engineering. The information extraction through optimization principles in computer vision lies at the heart of KBS. Most of the KBS problems applied to image analysis can be reduced into optimization processes. Under this methodology, information contained in the image is evaluated considering a knowledge base represented by a set of important quality characteristics. Then, by using a search strategy, the best image is detected. This image corresponds to the solution of the KBS problem.

Image enhancement (IE) is a computer vision task that can be approached as a KBS problem. It has attracted the attention of the computer vision community due to its multiple applications in areas such as medicine, security, transportation, etc [2–6]. IE is the process of improving the visual information contained in an image, increasing the difference among features of its different objects. The main objective is to improve the interpretability of the information present in an image for human viewers or make the enhanced image more suitable for further processing steps in any automatic computer vision system [6,7]. In general, IE methods modify pixel values through the histogram equalization, quadratic transformation, or fuzzy logic operation[2–4]. Among these techniques, histogram equalization (HE) [5,7–10] is the most used, simple and effective for image enhancement. HE considers the statistical features of pixels. In its operation, pixels relatively concentrated in positions of the histogram are redistributed over its whole scale. During this process, each existent intensity value A of the original image is mapped into another value B in the processed image without matter the number of pixels corresponding to A in the original image. Therefore, these

* Corresponding author.

E-mail addresses: alberto.lchang@academicos.udg.mx (A. Luque-Chang), erik.cuevas@cucei.udg.mx (E. Cuevas), marco.perez@cucei.udg.mx (M. Pérez-Cisneros), abraham.fausto@academicos.udg.mx (F. Fausto), arturo.valdivia@academicos.udg.mx (A. Valdivia-González), ramjucse@gmail.com (R. Sarkar).

schemes present an inadequate redistribution of the pixel data under the presence of noise or irrelevant small sets of pixels. As a consequence, these methods produce enhanced images with different problems such as the generation of undesirable artifacts and noise amplification [11–13].

In the last years, the problem of ICE has been approached through metaheuristic techniques as an alternative to design ICE schemes. Different from HE techniques, metaheuristic methods face the contrast enhancement problem from an optimization perspective. Therefore, under these methods, some aspects of the contrast enhancement process are related to an objective function whose optimal solution represents a good quality enhanced image. In general, contrast enhancement algorithms based in metaheuristic schemes have demonstrated to produce better results than those delivered by HE in terms of pixel intensity redistribution [3]. Some examples of these approaches include the use of Artificial Bee Colony (ABC) [14], Genetic Algorithms (GA) [12] and Particle Swarm Optimization (PSO) [15], Social Spider Optimization (SSO) [11,13], Cuckoo Search Algorithm (CS) [16], Firefly Algorithm (FFA) [17], Gravitational Search Algorithm (GSA) [18], Differential Evolution (DE) [19], among others. Although these methods have produced interesting image enhancement results, they present several flaws such as premature convergence to local optima and inability to maintain population diversity. In these methods, the redistribution of pixel data is evaluated through objective functions [12] that consider mainly heterogeneity. The more different pixel intensities are contained in the enhanced image, the more quality is the distribution. Under such conditions, these schemes present a limited effect of contrast enhancement in the presence of noise and irrelevant small set of pixels. This effect cannot be improved unless irrelevant visual information could be removed before the redistribution. Recently, new hybrid approaches that combine metaheuristic techniques with other computational schemes have been introduced in the literature for image contrast enhancement proposes. The objective of such methods is to increase the capacities of the metaheuristic approach through the incorporation of specific computational elements that provide additional information on the contrast enhancement process. Some representative examples include the algorithm Gamma-PSO proposed in [20], where the optimal values of a Gamma correction are determined by the PSO technique in order to enhance the contrast of a previously transformed image with a wavelet transform. Another interesting work is the Fuzzy-IPSO method reported in [21], where it is introduced an approach that combines fuzzy logic and PSO for enhancing the contrast of an image. Under this method, information of the histogram is obtained by a fuzzy system. With these data, the histogram is adjusted by the use of some weights computed through an improved version of the PSO algorithm.

The Moth Swarm Algorithm (MSA) [22] is a metaheuristic scheme inspired by the orientation of moths towards the moonlight. Different from other metaheuristic schemes, MSA considers three specific sub-populations. Therefore, according to the sub-population, each individual is conducted by using a different evolutionary operation, which represents a particular behavior of the moth insect. The incorporation of these operators in the search strategy reduces critical problems present in several metaheuristic algorithms, such as improper exploration-exploitation balance and premature convergence. Due to its interesting characteristics, MSA has been extensively applied in many complex engineering problems such as image processing [23], power systems [22], energy conversion [24], etc.

The presence of noise and small sets of pixel intensities in images often refers to the existence of ineffective/useless characteristics that maintain important image details hidden. Such elements correspond to sets of pixels that are too small to represent

objects or visible details in the image. This information contained in the image is not only adverse for human visualization, but also negatively influence the process of image enhancement. The elimination of this information represents a necessary method to improve the redistribution of the pixel data in the enhanced image. Therefore, relevant pixel intensities will be correctly highlighted in the redistribution since the space maintained for the eliminated pixel intensities can be reused. The Mean-shift algorithm [25] is a non-parametric technique commonly used to replace a characteristic \mathbf{x} scarcely existent in the feature space by an element \mathbf{x}^* densely contained within its neighborhood (local maximum). Under this scheme, starting at point \mathbf{x} , a new location is computed in the direction of the largest increase of the feature space until the local maximum \mathbf{x}^* has been reached. The simplicity and interesting properties of Mean-shift have extended its use in several domains such as regression [25] and clustering [26].

On the other hand, the Kullback–Leibler entropy (KL-entropy) [27,28], introduced by Kullback and Leibler, allows objectively evaluating the divergence between two different probability distributions. In general terms, the KL-entropy is used to assess how one probability distribution is different from a second probability considered as a reference. Its minimal value represents the complete dissimilarity between both distributions, while its maximal value corresponds to its best resemblance. Applications of the KL-entropy include the evaluation of the randomness in continuous time-series, the characterization of the relative (Shannon) entropy in information systems and the measurement of contained information when comparing different statistical models of inference. Different from other entropy formulations, the KL-entropy allows us to obtain no only the best possible data distribution in terms of the information content but also the distribution with the best similitude with regard to the original image data. Under such conditions, the results delivered by the use of KL-entropy involve images with enhanced contrast, also improving their human visual appearance (without distortion regarding the original information).

In this paper, an Image Contrast Enhancement (ICE) algorithm for images is introduced. Different from other approaches, the proposed ICE method considers the previous elimination of irrelevant sets of pixel intensities. The objective of this elimination is to reduce the number of histogram features in order to use the whole histogram range in the redistribution produced by the enhancement process. During this elimination process, the Mean-shift method is employed to delete unimportant small sets of pixels through the replacement of sporadic intensities by abundant features. Once obtained, the reduced histogram, the contrast improvement process, is performed. In this process, the Moth Swarm Algorithm (MSA) is adopted to redistribute the pixel intensities of the reduced histogram in the complete range so that the value of the Kullback–Leibler Entropy (KL-entropy) between a candidate distribution and the original information has been maximized. This paper presents three important contributions: (I) The use of an elimination process to reduce the number of histogram features in order to improve the pixel intensity redistribution. Without consideration of this process, the level of contrast enhancement reached is very limited. According to our best knowledge, no comprehensive study has considered the elimination process of irrelevant information to improve the redistribution process within an ICE scheme. (II) The incorporation of the KL-entropy for the redistribution process. Though its inclusion, images with a better human visual appearance are produced. (III) The use of the Moth Swarm Algorithm (MSA) to find the best redistribution that represents the best-enhanced image. The search characteristics of this scheme allow exploring the solution space without presenting the associate problems of other

metaheuristic schemes. The performance of the proposed scheme has been tested considering a number of representative datasets commonly found in the literature. Its results are also compared with those produced by other well-known similar techniques. Experimental results suggest that the proposed method has a better performance in comparison with other schemes in terms of several performance indexes.

The rest of the paper is organized as follows: In Section 2, a brief explanation of the Mean-shift algorithm is given; in Section 3, the main characteristics of the ICE problem are illustrated; in Section 4, the most important elements about the MSA are presented; in Section 5, the proposed approach is presented; Section 6 exhibits the experimental results; finally, in Section 7, conclusions are drawn.

2. Mean-shift algorithm

The Mean-shift method [25] is a non-parametric scheme commonly used to reduce unimportant information contained in a dataset. Under this algorithm, a characteristic \mathbf{x} scarcely present in the feature space is replaced by other \mathbf{x}^* densely contained within its neighborhood (local maximum). The operation of the Mean-shift starts at a random point \mathbf{x} within the density feature map. Then, a new location is computed in the direction of the largest increase of the density feature space until the local density maximum \mathbf{x}^* has been reached. Two processes integrate the Mean-shift scheme. First, a Kernel function is applied to estimate the probability density function (PDF) of the data. Then, an optimization step based on gradient ascent is conducted to find the local maxima (density attractors) over the PDF [29].

2.1. Probability density function estimation

In the mean-shift algorithm, the probability density function is estimated defining some non-negative, symmetric kernel function K , such that:

$$K(\mathbf{x}) \geq 0; \quad K(-\mathbf{x}) = K(\mathbf{x}); \quad \int K(\mathbf{x})d\mathbf{x} = 1 \quad (1)$$

Assuming a set of n features $\mathbf{x}_1, \mathbf{x}_2, \dots, \mathbf{x}_n$, the density function $\hat{f}(\mathbf{x})$, can be estimated in terms of K as follows:

$$\hat{f}(\mathbf{x}) = \frac{1}{nh} \sum_{i=1}^n K\left(\frac{\mathbf{x} - \mathbf{x}_i}{h}\right), \quad (2)$$

where h represents the influence area of K .

2.2. Density attractors

The main idea behind the estimation of a PDF for a given dataset is to find characteristic points \mathbf{x}^* which better represent the distribution of the modeled data points. These points are represented by the local maxima present in the estimated PDF $\hat{f}(\mathbf{x})$. Such points can be found by applying a gradient-based optimization method. In this scheme, a random point \mathbf{x} is first defined. Then, a new location is computed in the direction of the density gradient $\nabla \hat{f}(\mathbf{x})$ until the local maximum \mathbf{x}^* has been reached. This update rule is formulated as follows:

$$\mathbf{x}^{t+1} = \mathbf{x}^t + \delta \cdot \nabla \hat{f}(\mathbf{x}^t), \quad (3)$$

where t denotes the current iteration number, while δ represents the step size. Under this formulation, the density gradient at any point \mathbf{x} is calculated by computing the derivative of the PDF as follows:

$$\nabla \hat{f}(\mathbf{x}) = \frac{\partial}{\partial \mathbf{x}} \hat{f}(\mathbf{x}) = \frac{1}{nh} \sum_{i=1}^n \frac{\partial}{\partial \mathbf{x}} K\left(\frac{\mathbf{x} - \mathbf{x}_i}{h}\right) \quad (4)$$

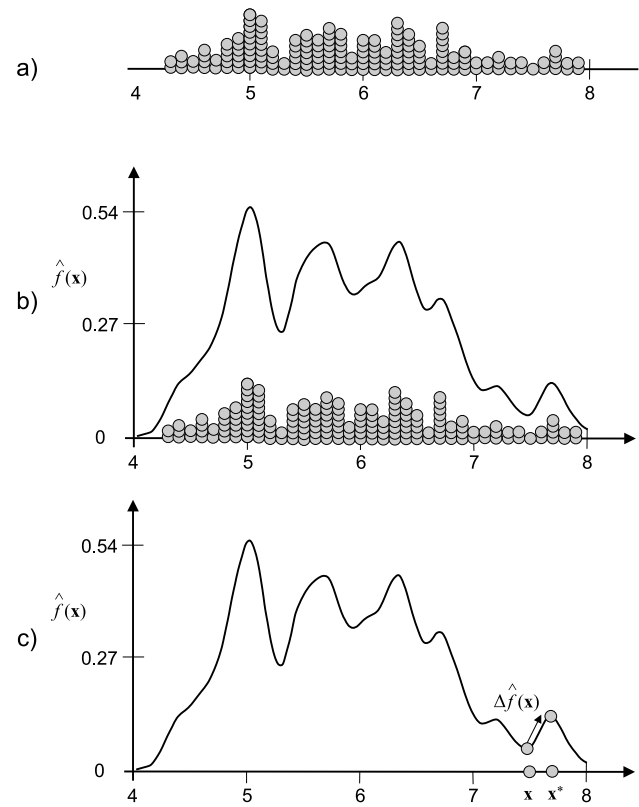


Fig. 1. Illustration of the mean-shift process. (a) dataset example, (b) estimated PDF $\hat{f}(\mathbf{x})$ from Eq. (2) and (c) replacing \mathbf{x} by \mathbf{x}^* as a consequence of the density gradient operation.

Fig. 1 is an illustration of the mean-shift process. Considering that **Fig. 1(a)** represents the dataset, **Fig. 1(b)** shows the estimated PDF $\hat{f}(\mathbf{x})$ from Eq. (2). Then, starting at point \mathbf{x} , a new location is computed in the direction of the largest increase of the feature space until the local maximum \mathbf{x}^* has been reached. Therefore, the feature \mathbf{x} of low density is replaced by \mathbf{x}^* which represents a neighbor representative feature.

3. Image contrast enhancement through optimization

An optimization-based contrast enhancement approach relates some aspects of the contrast enhancement process to an objective function. Under such conditions, obtaining the minimal or maximal value of this objective function, it is found the image with the best possible contrast enhancement characteristics in terms of the elements used for the construction of the objective function. Under these schemes, it is coded a set of alternative histogram distributions as decision variables to determine hypothetical solutions to the contrast enhancement problem. Each histogram is represented by a vector of 256 dimensions. An objective function evaluates the quality of the enhancement produced by each hypothetical histogram. Therefore, conducted by the values of the objective function, the set of encoded histograms is operated through a particular metaheuristic approach so that the solutions (histograms) are iteratively improved in each generation of the optimization process. In general, a contrast enhancement task involves the maximization of the objective function, the lower the index, the better is the improved result.

Fig. 2 illustrates the enhancement process under an optimization approach. In the figure, a solution A , is modified by the operators of the optimization approach. As a consequence of this modification, a new solution B is produced. The new solution B

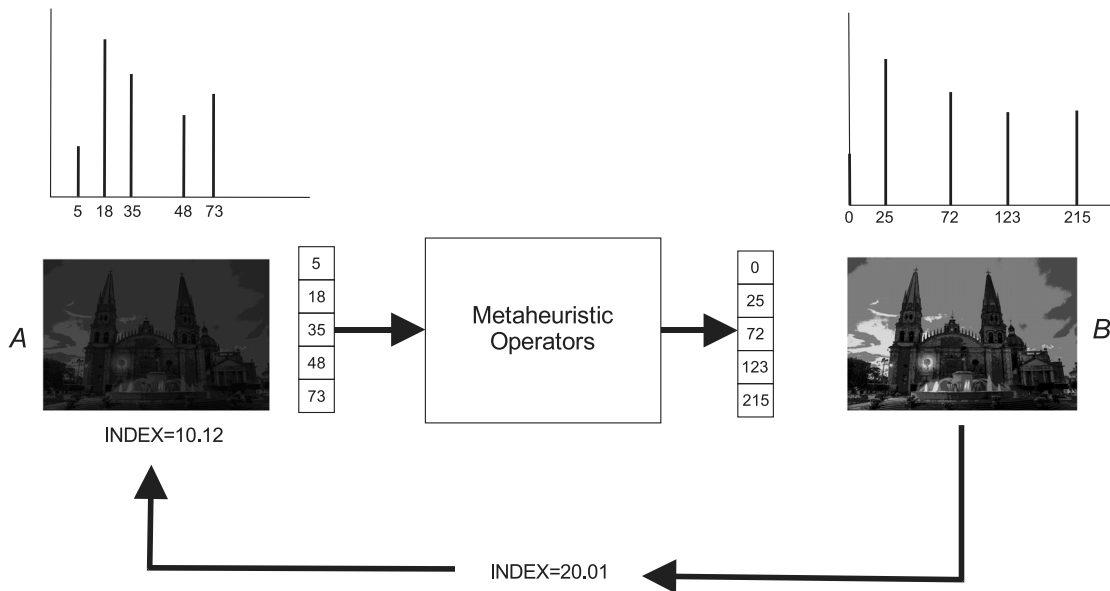


Fig. 2. Illustration of the enhancement process under an optimization approach.

presents a better enhancement index according to its evaluation of the objective function.

4. Moth swarm algorithm

The MSA [22] is a recent swarm algorithm designed to solve global optimization problems. In MSA, the swarm population is divided into three groups: Pathfinders, Prospectors and Onlookers. The following subsections are summarized the complete MSA algorithm. For more details, refer to [22].

4.1. Initialization

In the MSA approach, the population involves a set of p individual moths $\mathbf{M} = \{\mathbf{m}_1, \mathbf{m}_2, \dots, \mathbf{m}_p\}$, where $\mathbf{m}_i = [m_{i,1}, m_{i,2}, \dots, m_{i,n}]$ represents a candidate solution. During the initialization, the search agents assume random positions according to the following model:

$$m_{ij} = \text{rand}(0, 1) \cdot (m_j^{\max} - m_j^{\min}) + m_j^{\min} \quad (5)$$

$$\forall i \in \{1, 2, \dots, p\}, \quad j \in \{1, 2, \dots, n\}$$

where, m_j^{\max} and m_j^{\min} are the upper and lower limits of the search space.

4.2. Recognition phase

In this phase, two operators are applied to each candidate solution: crossover and Lévy perturbation [30]. The crossover point is defined through the following formulation:

$$\mu_j^i = \frac{\sqrt{\frac{1}{p_n} \sum_{a=1}^{p_n} (m_{aj}^i - \bar{m}_j^i)^2}}{\bar{m}_j^i} \quad \bar{m}_j^i = \frac{1}{p_n} \sum_{a=1}^{p_n} m_{aj}^i \quad (6)$$

with p_n is the number of pathfinder moths. Under such conditions, the new solution is computed as follows:

$$\vartheta^i = \frac{1}{n} \sum_{j=1}^n \mu_j^i \quad (7)$$

4.2.1. Lévy flights

The MSA uses the Lévy perturbations [30] to generate random steps. Therefore, to generate a Lévy L_i random sample the Mantegna's algorithm [31] is used. This scheme can be described as follows:

$$L_i \sim \text{scale} \oplus \text{Lévy}(\alpha) \sim 0.01 \frac{v}{|z|^{\frac{1}{\alpha}}}, \quad (8)$$

where $\alpha \in [0, 2]$, scale is the dispersion size, \oplus is the entrywise multiplication, $v = N(0, \mu_v)$ and $z = N(0, \mu_z)$ are two normal distributions.

4.2.2. Lévy Mutation

For nc operations ($nc \in cp$), the algorithm creates a sub-trial vector $\vec{x}_p = [x_{p1}, x_{p2}, \dots, x_{pn_c}]$ as follows:

$$\vec{x}_p^i = L_1^i * \left(\vec{m}_{r_2}^i, - \vec{m}_{r_3}^i \right) + L_2^i * \left(\vec{m}_{r_4}^i, - \vec{m}_{r_5}^i \right) \quad (9)$$

$$\forall r^1 \neq r^2 \neq r^3 \neq r^4 \neq r^5 \neq p \in \{1, 2, \dots, np\} m_{r_1}^i,$$

where L_1 and L_2 are two independent Lévy random samples [31].

4.2.3. Adaptive crossover

Each pathfinder updates its position combining crossover operations and mutated variables. Therefore, this trail/mixed solution Tms_{pj}^i for the element i is described as follows:

$$Tms_{pj}^i = \begin{cases} \vec{x}_{pj}^i & \text{if } j \in cp \\ \vec{m}_{pj}^i & \text{if } j \notin cp \end{cases} \quad (10)$$

4.2.4. Selection strategy

Once the adaptive crossover operator is complete, the fitness value of the complete trail solution is calculated and compared with its corresponding host solution. Then, a set of np solutions are selected following the roulette scheme [22].

4.3. Transversal flight

The group of elements with the best luminescence intensities is considered as prospectors in the next iteration. On the course

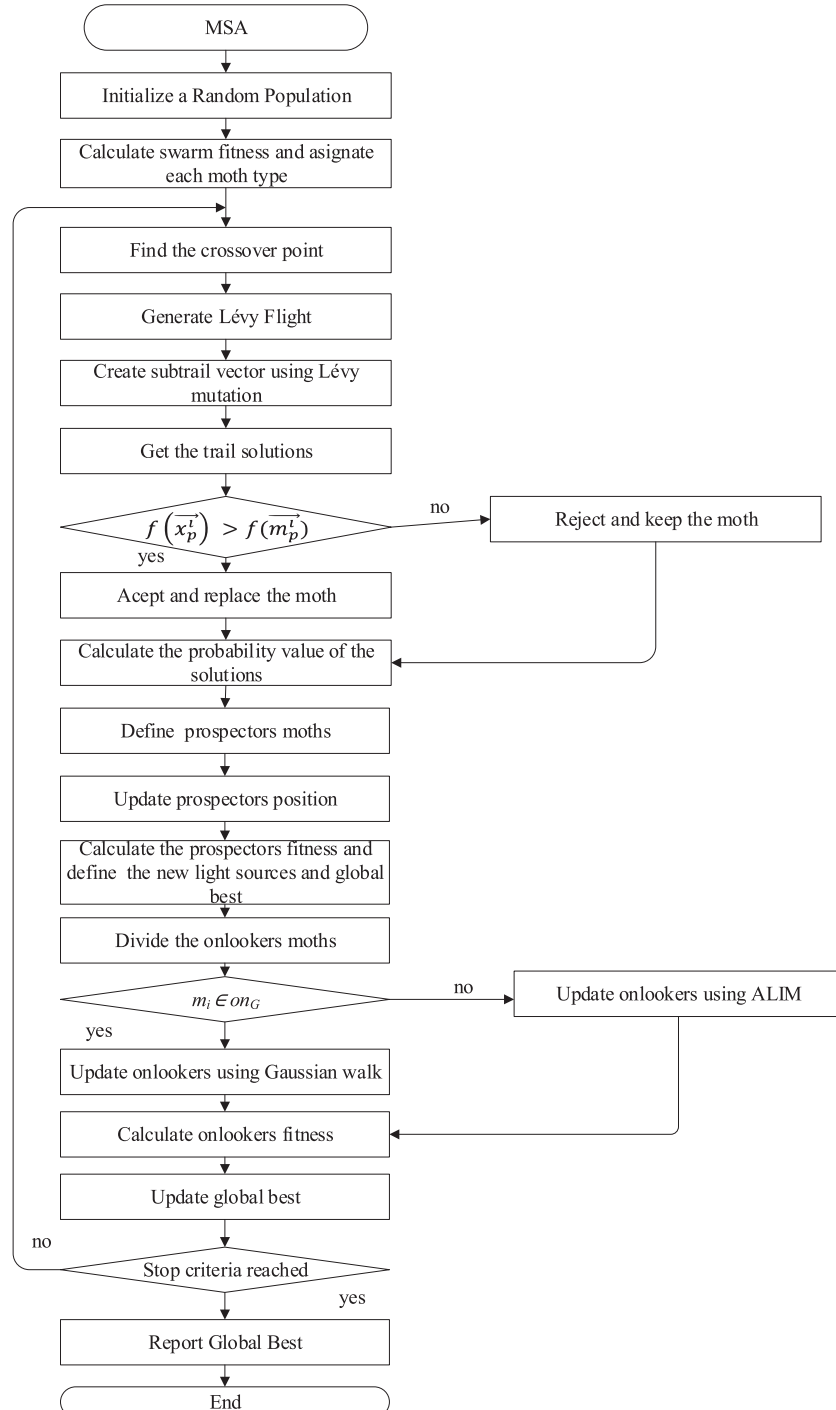


Fig. 3. The flowchart of the MSA algorithm.

of the optimization process, the prospectors number pf decreases as follows:

$$pf = \text{round} \left((p - p_n) \times \left(1 - \frac{i}{i_c} \right) \right), \quad (11)$$

where i_c is the current iteration number.

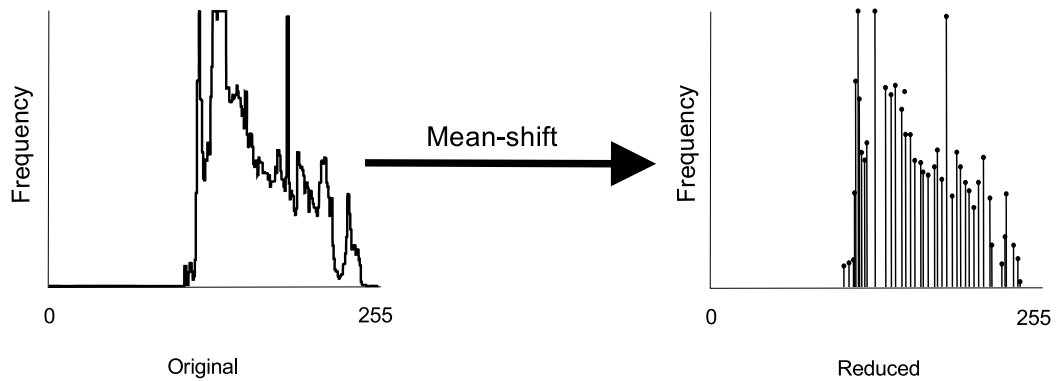
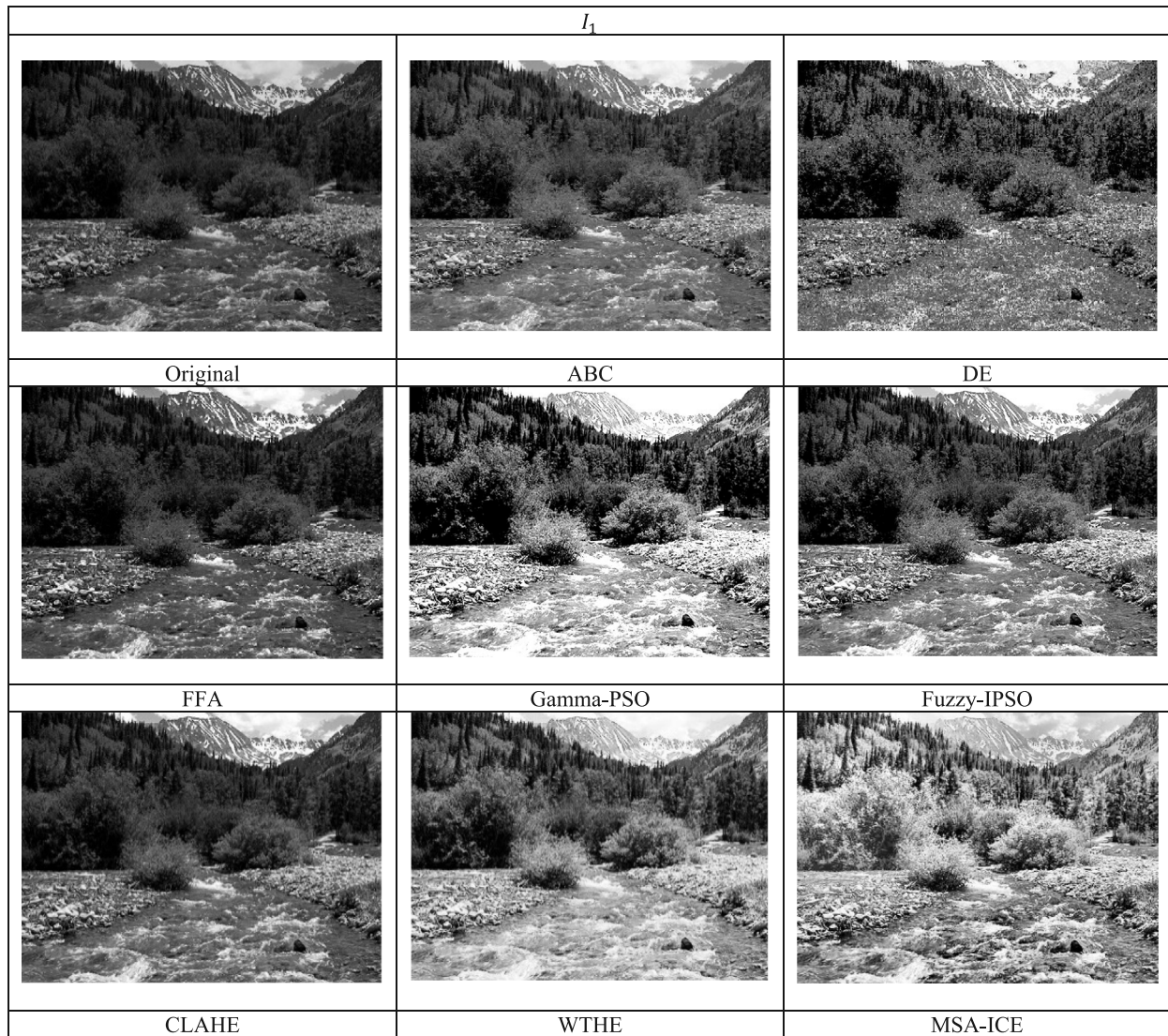
4.4. Celestial navigation

During the optimization process, the decreasing prospectors number increases the onlookers number ($o_n = p - p_n - pf$). This

may lead to a fast increment on the convergence rate. The moths with the lower luminescent sources in the swarm are considered onlookers. In this phase, onlookers search exhaustively near to prospectors elements. The onlookers are divided into two equal parts.

4.4.1. Gaussian walks

In this phase, with the objective of exploiting promising areas on the search space, a stochastic Gaussian distribution is used to perturb original positions. Therefore, the new onlooker positions

**Fig. 4.** Reduction of grayscale intensities produced by the mean-shift.**Fig. 5.** Contrast enhancement results of the image I_1 for ABC, DE, FFA, Gamma-PSO, Fuzzy-IPSO, CLAHE, WTHe and MSA-ICE methods.

(for the first sub-set) are computed as follows:

$$m_o^{i+1} = m_o^i + \varepsilon_1 + [\varepsilon_2 \times \text{best} - \varepsilon_3 \times m_o^i]; \quad \forall o \in [1, 2, \dots, on_G] \quad (12)$$

where, ε_1 is a random sample drawn from the Gaussian distribution while ε_2 and ε_3 are random uniform numbers $\in [0, 1]$.

4.4.2. Associative learning mechanism with immediate memory (ALIM)

The second onlookers sub-set with size $on_A = o_n - on_G$ moves towards the global best according to immediate memory. This memory is initialized from a continuous uniform Gaussian distribution on the interval from $m_o^i - m_o^{\min}$ to $m_o^{\max} - m_o^i$. Therefore,



Fig. 6. Contrast enhancement results of the image I_2 for ABC, DE, FFA, Gamma-PSO, Fuzzy-IPSO, CLAHE, WTHE and MSA-ICE methods.

the new positions are computed as follows:

$$\begin{aligned} m_o^{i+1} = & m_o^i + 0.001 \cdot G [m_o^i - m_o^{\min}, m_o^{\max} - m_o^i] \\ & + \left(1 - \frac{g}{G}\right) \cdot r_1 \cdot (pbest^i - m_o^i) \\ & + \frac{2g}{G} \cdot r_2 \cdot (gbest^i - m_o^i), \end{aligned} \quad (13)$$

where $o \in [1, 2, \dots, o_n]$, $2g/G$ is the social factor, $1 - (g/G)$ is the cognitive factor, r_1 and r_2 are two random numbers $\in [0, 1]$ and $pbest$ is a light source randomly chosen from the new pathfinders group based on the probability value p_{v_p} of its corresponding solution. The flowchart of the MSA algorithm is shown in Fig. 3.

5. CS-MSA-Based image contrast enhancement via gray-levels mapping

The purpose of contrast enhancement on images is to define an appropriate distribution, which allows a better visualization in comparison with the original image. The existence of noise and small sets of pixel intensities affect the process of image enhancement negatively. The presence of such elements does not allow the adjustment of the original image distribution in the complete range.

In this paper, the proposed approach, called MSA-ICE, divides the image contrast enhancement process into two steps. In the first step, an elimination process is conducted for replacing sporadic pixel intensities in the original histogram by abundant intensities in the histogram. This process is achieved by the Mean-shift algorithm. In the second step, the contrast of the reduced histogram is adjusted. For this propose, the Moth Swarm Algorithm (MSA) is used. Under this process, the elements of the reduced histogram are redistributed so that the new distribution maximizes an objective function characterized by the Kullback-Leibler Entropy (KL-entropy).

5.1. Data elimination

During this process, under the application of the mean-shift algorithm, features of low density are replaced with elements of higher presence in the feature space. As a result, the number of gray levels in the image is reduced. Therefore, noise and small sets of pixel intensities that affect the enhancement process are eliminated. Fig. 4 shows the result of this reduction.

In this paper, to estimate the probability density function, the quadratic Kernel function is employed. It is defined as follows:

$$K(x) = \left(\frac{15}{16}\right) \cdot (1 - x^2)^2 \quad (14)$$



Fig. 7. Contrast enhancement results of the image I_3 for ABC, DE, FFA, Gamma-PSO, Fuzzy-IPSO, CLAHE, WTHE and MSA-ICE methods.

Under this operation, it is assumed an original histogram H_0 defined as:

$$H_0 = \{p_0, p_1, \dots, p_{L-1}\}, \quad p_r = \frac{n_r}{m \cdot n}, \quad r \in (0, 1, \dots, L-1) \quad (15)$$

where L represent the number of grayscale intensities and n_r refers to the number of pixels with intensity r . $m \cdot n$ symbolizes the image dimensions. Therefore, the reduced histogram $H_R = \{q_0, q_1, \dots, q_{L-1}\}$ is produced through the operation of the mean-shift method over H_0 . In the scheme, starting with each pixel intensity i , the mean-shift algorithm finds the pixel j that represents its local maxima. Under such conditions, the components i and j of the reduced histogram H_R are computed such as the $q_j = p_j + p_i$ while q_i is set to zero. With this operation, the pixels of intensity i in the image are assumed as pixels of intensity j .

5.2. Objective function

In contrast improvement, the Moth Swarm Algorithm (MSA) is used to adjust the pixel intensities of the reduced histogram H_R . To evaluate the quality of the contrast enhancement, the

following objective function is employed:

$$J_P(H_R) = \log(\log e_i(I)) \cdot \frac{e_p(I)}{hp^*vp} \cdot KL_e(I) \quad (16)$$

J_P incorporates different image characteristics that are considered important in the context of image enhancement. It includes: (1) the number of edge pixels $e_p(I)$ (detected on an image processed by applying a Sobel filter), (2) the total sum of the intensity edge pixels $e_i(I)$, (3) the image resolution hp^*vp , and (4) the symmetric Kullback-Leibler entropy $KL_e(I)$ [27,28] between the original and reduced images, which is defined as follows:

$$KL_e(I) = \sum h_1 \cdot \log \frac{h_1}{h_2} + \sum h_2 \cdot \log \frac{h_2}{h_1} \quad (17)$$

where h_1 and h_2 are the histograms of the original and the reduced image respectively.

The objective function J_P combines the number of edge pixels $e_p(I)$, the intensity of edge pixels $e_i(I)$ and Kullback-Leibler entropy $KL_e(I)$ of the image. The elements $e_p(I)$ and $e_i(I)$ determine the amount and magnitude of important characteristics presented in the enhanced image. Their value is associated with the quality of the fine details contained in the enhanced image. On the other hand, the $KL_e(I)$ value evaluates the resemblance between the original h_1 and the enhanced image h_2 respectively. Under such



Fig. 8. Contrast enhancement results of the image I_4 for ABC, DE, FFA, Gamma-PSO, Fuzzy-IPSO, CLAHE, WTHe and MSA-ICE methods.

conditions, the values of J_p are used to identify the enhanced image with the most content of fine details, but preserving the structural characteristics of the original image.

5.3. Penalty function

In the contrast enhancement process, pixel intensities of the reduced histogram H_R are relocated in positions that improve the image visualization. The new positions are distributed in the same order so that they cover the whole grayscale. Under these conditions, the pixel intensity i is always located previously to intensity $i + 1$. During the optimization process, produced candidate solutions can be inconsistent. This inconsistency is provoked when a pixel intensity is $i + 1$ is redistributed in a previous location to the pixel intensity i . To avoid this problem, a penalty function that numerically punishes the solutions with such inconsistencies is defined. Therefore, the problem of enhancement contrast can be formulated as a constrained optimization task as follows:

$$\begin{aligned} & \max \text{Fit}(H_R) \\ & \text{subject to: } q_i < q_{i+1}, \forall i \in (0, 1 \dots, L - 1) \end{aligned} \quad (18)$$

Under this formulation, the function $\text{Fit}(H_R)$ is defined such as:

$$\text{Fit}(H_R) = \begin{cases} \text{fit}(H_R), & \text{in case of inconsistency} \\ P_e(H_R), & \text{otherwise} \end{cases} \quad (19)$$

where $P_e(H_R)$ is the penalty function that directly affects the fitness function defined in Eq. (25). The value of $P_e(H_R)$ increases with the number of produced inconsistencies. $P_e(H_R)$ can be formulated as follows:

$$P_e(H_R) = (\text{NVC} + \text{SVC}) * \text{PC} \quad (20)$$

NVC is the number of produced inconsistencies. PC is a constant defined as a high value, which ensures a functional penalization. SVC considers the sum of all pixel elements n_d involved in the inconsistency d :

$$\text{SVC} = \sum_{d=1}^{\text{NVC}} \max \{0, n_d\} \quad (21)$$

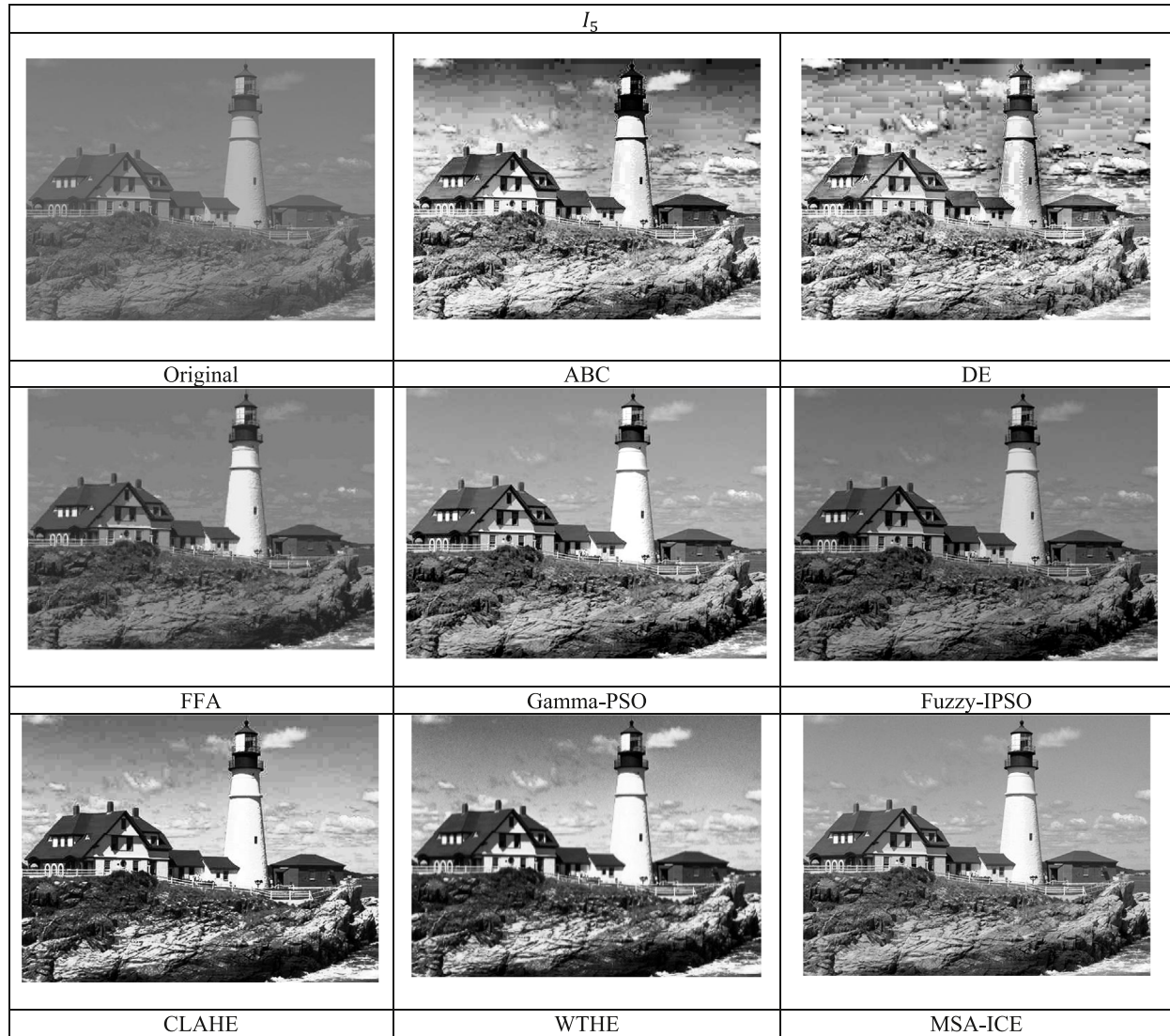


Fig. 9. Contrast enhancement results of the image I_5 for ABC, DE, FFA, Gamma-PSO, Fuzzy-IPSO, CLAHE, WTHe and MSA-ICE methods.

Table 1

Average performance results of ABC, DE, FA, Gamma-PSO, Fuzzy-IPSO, CLAHE, WTHe and MSA-ICE in terms of the indexes SSIM, MSE, EPI, E, REC and RR for all images from the CSIQ dataset.

Index	ABC	DE	FFA	Gamma-PSO	Fuzzy-IPSO	CLAHE	WTHe	MSA-ICE
SSIM	0.7412	0.5874	0.6847	0.7502	0.7598	0.7021	0.7157	0.8620
MSE	5.88E+03	6.51E+03	6.31E+03	5.80E+03	5.77E+03	6.22E+03	6.15E+03	5.22E+03
EPI	1.1132	0.9721	1.1031	1.0021	1.0254	1.0014	1.0997	1.2491
E	6.0141	4.8741	5.8741	6.0982	6.0098	5.5721	5.7864	6.3871
REC	1.0964	0.9847	1.0101	1.0782	1.0320	1.0004	1.0089	1.1272
RR	39.4714	27.214	36.4124	39.0088	38.9801	30.0087	30.8714	43.0121

Table 2

Average performance results of ABC, DE, FA, Gamma-PSO, Fuzzy-IPSO, CLAHE, WTHe and MSA-ICE in terms of the indexes SSIM, MSE, EPI, E, REC and RR for all images from the TID2013 dataset.

Index	ABC	DE	FFA	Gamma-PSO	Fuzzy-IPSO	CLAHE	WTHe	MSA-ICE
SSIM	0.6784	0.4914	0.6210	0.6708	0.6921	0.6107	0.6521	0.7421
MSE	6.21E+03	7.18E+03	6.91E+03	6.20E+03	6.19E+03	7.07E+03	6.73E+03	6.08E+03
EPI	1.0974	0.9974	1.0087	1.0021	1.0198	1.0004	1.0241	1.1987
E	5.8041	5.4170	5.6127	5.8421	5.9001	5.5496	5.7410	6.1047
REC	1.0021	0.9784	0.9974	0.9997	1.0087	0.9870	1.0007	1.0975
RR	37.4120	21.0745	25.7412	37.2104	38.0078	31.7847	27.8741	41.2101

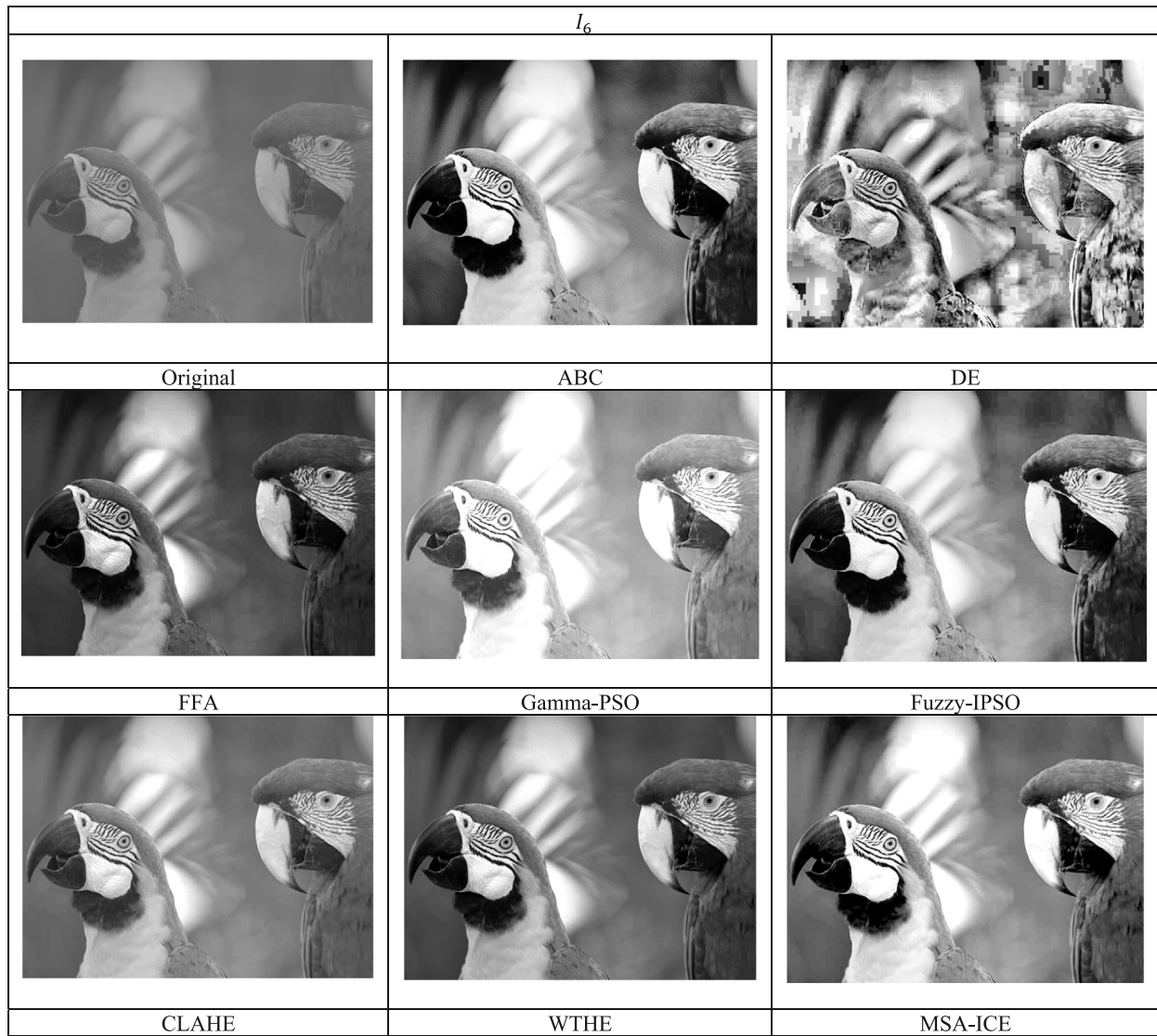


Fig. 10. Contrast enhancement results of the image I_6 for ABC, DE, FFA, Gamma-PSO, Fuzzy-IPSO, CLAHE, WTHe and MSA-ICE methods.

6. Experimental results

In order to evaluate the performance of the proposed MSA-ICE approach, a set of representative experiments has been conducted. In the experiments, the images contained in the datasets of CSIQ [32] and TID2013 [33] have been used. The CSIQ dataset contains 116 different images that have been produced by modifying the contrast at different levels of 30 images considered as references. The dataset TID2013 involves 250 images distributed in 10 distinct groups of images produced from 25 reference images. Each group in the TID2013 dataset considers a different type of contrast.

Six performance indexes have been considered in our analysis: Structural similarity index measurement (*SSIM*), Mean squared error (*MSE*), Edge Preserve Index (*EPI*), Entropy (*E*), Relative Enhancement Contrast (*REC*), Range Redistribution (*RR*) and Computational Complexity (*CC*). The first six indexes evaluate the quality of the produced image while the last one measures the computational effort. These indexes have been adopted in order to be compatible with other works.

To calculate the different indexes, it is considered an original image, with an unsatisfactory contrast defined as **R**. This image is used as input of an ICE method. As a result, an enhanced image **I**

is generated. Therefore, the Structural similarity index measurement (*SSIM*) [34] evaluates the similarity between the improved image **I** and the original **R**. Assuming that $\{p_1, \dots, p_{M \times N}\}$ represents the data pixel of **I** and $r_1, \dots, r_{M \times N}$ the original data, the *SSIM* is computed as follows:

$$SSIM = \frac{(2\mu_I\mu_R + Q_1)(2\sigma_{IR} + Q_2)}{(\mu_I^2 + \mu_R^2 + Q_1)(\sigma_I^2 + \sigma_R^2 + Q_2)} \quad (22)$$

where Q_1 and Q_2 symbolize two small positive constants (typically 0.01). μ_I and μ_R correspond to the mean values of the segmented and reference data, respectively. σ_I and σ_R represent the variance of the segmented and reference data, respectively. σ_{IR} is the covariance of both data elements **I** and **R**. The values produced by *SSIM* ranges from 0 to 1.

The *MSE* evaluates the similarity between a segmented image **I** and its reference **R** by subtracting the pixel values of the segmented image with the pixels of its reference and then computing the mean value of the total error. The RMS is obtained by using the following model:

$$MSE = \frac{1}{MN} \sum_{i=1}^M \sum_{j=1}^N (\mathbf{I}(i,j) - \mathbf{R}(i,j))^2 \quad (23)$$



Fig. 11. Set of the representative color images considered in the experiments extracted from CSIQ and TID2013 databases.. (For interpretation of the references to color in this figure legend, the reader is referred to the web version of this article.)

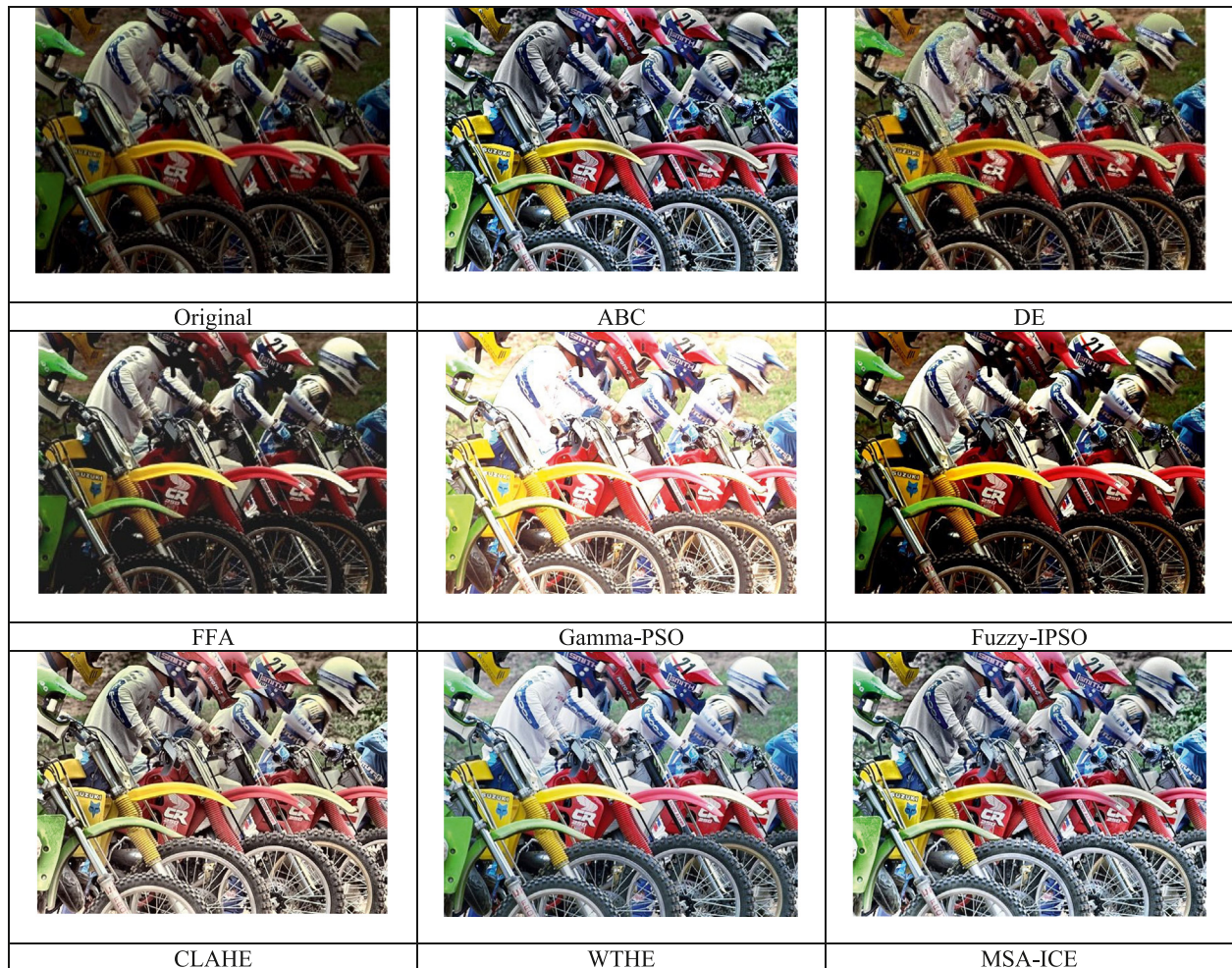


Fig. 12. Contrast enhancement results of the color image IC_1 for ABC, DE, FFA, Gamma-PSO, Fuzzy-IPSO, CLAHE, WTHE and MSA-ICE methods.. (For interpretation of the references to color in this figure legend, the reader is referred to the web version of this article.)



Fig. 13. Contrast enhancement results of the color image IC_2 for ABC, DE, FFA, Gamma-PSO, Fuzzy-IPSO, CLAHE, WTHE and MSA-ICE methods.. (For interpretation of the references to color in this figure legend, the reader is referred to the web version of this article.)

Edge Preserve Index (EPI) [35] evaluates the conservation of the edges in the enhanced image \mathbf{I} with regard to the original image \mathbf{R} . A high EPI value corresponds to better algorithm performance. The value of EPI is computed as follows:

$$EPI = \frac{\sum_{i=1}^M \sum_{j=1}^N |\mathbf{I}(i, j) - \mathbf{I}(i, j + 1)| + |\mathbf{I}(i, j) - \mathbf{I}(i + 1, j)|}{\sum_{i=1}^M \sum_{j=1}^N |\mathbf{R}(i, j) - \mathbf{R}(i, j + 1)| + |\mathbf{R}(i, j) - \mathbf{R}(i + 1, j)|} \quad (24)$$

The Entropy (E) assesses the information content of the enhanced image \mathbf{I} . E is a quality measurement that indirectly evaluates the number of details existent in \mathbf{I} . A larger value of E corresponds to more information content in \mathbf{I} . The index E is calculated with the following model:

$$E = - \sum_{i=0}^{L-1} P(q) \cdot \log(P(q)) \quad (25)$$

Where $P(q)$ refers to the probability density function at the intensity level q ($q \in 0, \dots, L - 1$) of the image \mathbf{I} . L symbolizes the total number of grayscale levels represented in \mathbf{I} .

The Relative Enhancement Contrast (REC) [36] allows us to quantify the contrast difference between the enhanced image \mathbf{I} and the original \mathbf{R} . The value of REC gives an evaluation of the intensity differences among the multiple objects and structures contained in \mathbf{I} and \mathbf{R} . A high value of REC corresponds to a better-enhanced image. The REC index is obtained by the following

formulation:

$$REC = 20 \cdot \log \left[\frac{1}{M \times N} \sum_{i=1}^M \sum_{j=1}^N (\mathbf{I}(i, j))^2 - \left(\frac{1}{M \times N} \sum_{i=1}^M \sum_{j=1}^N \mathbf{R}(i, j) \right)^2 \right] \quad (26)$$

The Range Redistribution (RR) [37] index determines the way in which pixel intensities are distributed in the improved image \mathbf{I} . RR is computed through the following expression:

$$RR = \frac{1}{M \times N \cdot (M \times N - 1)} \sum_{q=1}^{L-1} \sum_{r=q}^{L-1} P(q) P(r) (r - q) \quad (27)$$

where $P(q)$ and $P(r)$ refer to the probability density functions at the intensity levels q and r , respectively, ($q, r \in 0, \dots, L - 1$) of the image \mathbf{I} . L symbolizes the total number of grayscale levels represented in \mathbf{I} . A high value of RR means that the histogram of \mathbf{I} is better distributed without presenting intensity concentrations.

The ICE methods considered in the experiments are in general, complex processes with several random operations and stochastic sub-routines. Therefore, it is impractical to conduct a complexity analysis from a deterministic point of view. For this reason, the computational complexity (CC) is evaluated considering the computational effort in seconds invested for each algorithm.

The experimental results are divided into four subsections. In the first Section 6.1, the performance of the proposed MSA-ICE is

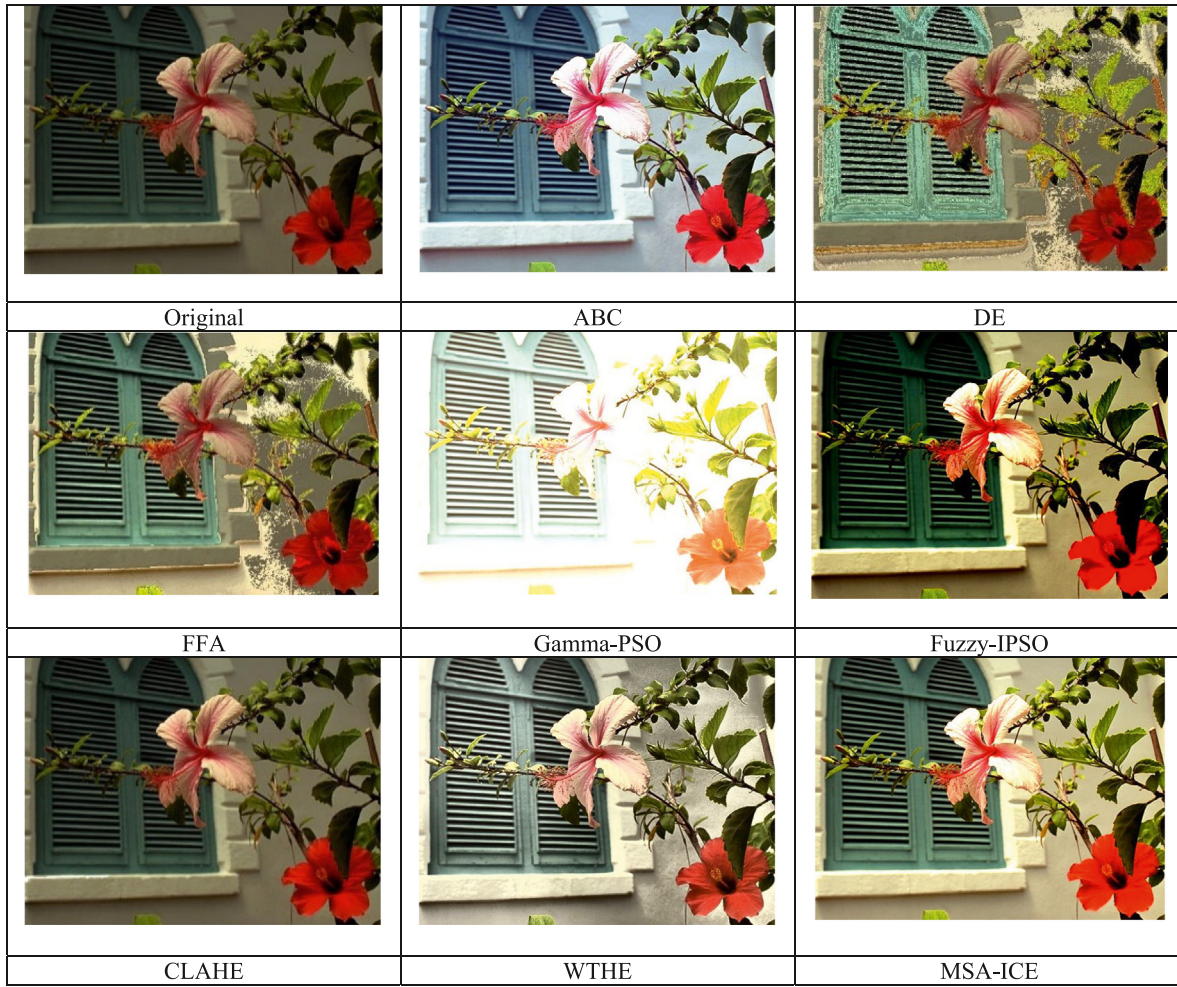


Fig. 14. Contrast enhancement results of the color image IC_3 for ABC, DE, FFA, Gamma-PSO, Fuzzy-IPSO, CLAHE, WTHE and MSA-ICE methods.. (For interpretation of the references to color in this figure legend, the reader is referred to the web version of this article.)

evaluated in terms of $SSIM$, MSE , EPI , E , REC , RR , CC with regard to grayscale images. In the second Section 6.2, the enhancement contrast results produced by the proposed objective function J_P (Eq. (16)) based on the KL-entropy are compared with those produced by other objective functions used in the literature for contrast enhancement. In the third Section 6.3, a comparative study among the ICE metaheuristic methods is accomplished. In the fourth Section 6.4, the results of MSA-ICE are extended for color images.

6.1. Comparison over grayscale images in terms of $SSIM$, MSE , EPI , E , REC , RR and CC

In this subsection, the performance of our proposed MSA-ICE scheme is analyzed considering grayscale images. In the experiments, the MSA-ICE is applied to all the images contained in the datasets of CSIQ, TID2013. Its results are also compared with those produced by similar schemes based on metaheuristic methods such as the Artificial Bee Colony (ABC) algorithm [14], Differential Evolution (DE) [38] and Firefly Algorithm (FFA) [17]. In all comparisons, the population size has been set to $N = 30$, while the maximum number of iterations is set to $k_{\max} = 100$. Such a stop criterion has been selected in order to keep compatibility to other similar works reported on the literature [39].

The specific parameter setup for each metaheuristic scheme is described as follows:

- ABC: The algorithm is implemented by setting the parameter $limit = \text{num Of Food Sources} * \text{dims}$, where $\text{num Of Food Sources} = N$ (population size) and $\text{dims} = n$ (dimensionality of the solution space) [14].
- DE: The crossover rate is set to $CR = 0.5$, while the differential weight is given as $F = 0.2$ [38].
- FFA: The randomness factor and light absorption coefficient are set to $\alpha = 0.2$ and $\gamma = 1.0$, respectively [17].
- MSA: The number of sub-trial vectors is set to $nc = 8$.

In the comparisons, it has also been considered two recent hybrid approaches, such as the Gamma-PSO algorithm [20] and the Fuzzy-IPSO method [21]. Moreover, two classical algorithms based on histogram equalization, such as the Local and Adaptive Histogram Equalization (CLAHE) [8] and the Weighted thresholded Histogram Equalization (WTHE) [9] have also been included in the analysis. All the algorithms have been configured with the same parameter values selected in their references. All these parameters are kept with no modifications during all experimental work. The selected parameter configurations represent, according to their own references, the best possible performance of each corresponding technique. All experiments were performed on MatLab® R2016a, running on a computer with an Intel® Core™ i7-3.40 GHz processor, and Windows 8 (64-bit, 8 GB of memory) as its operating system.

When the pixel intensities of an image are highly concentrated in a region (low contrast), its fine details could be lost. With

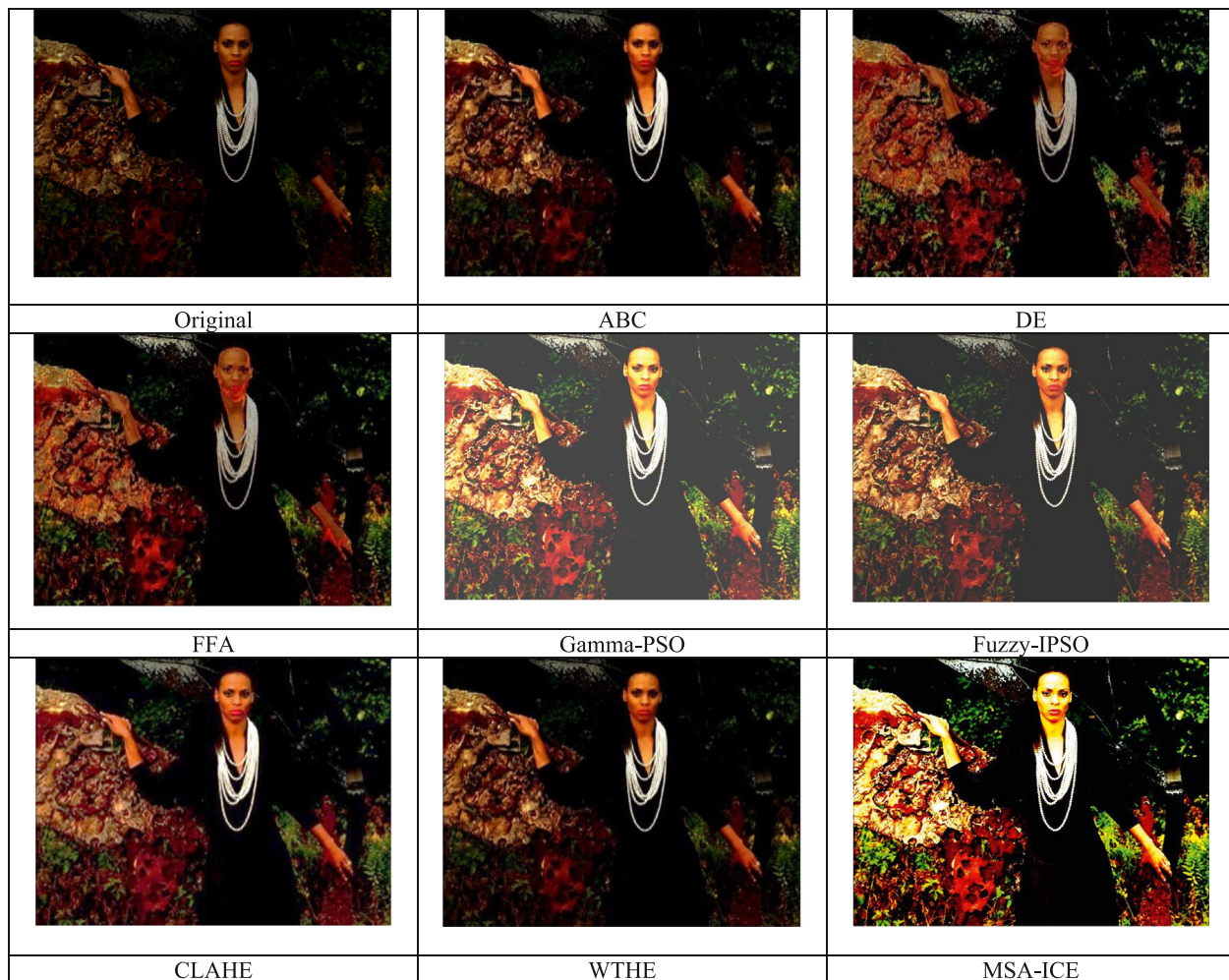


Fig. 15. Contrast enhancement results of the color image IC_4 for ABC, DE, FFA, Gamma-PSO, Fuzzy-IPSO, CLAHE, WTHE and MSA-ICE methods.. (For interpretation of the references to color in this figure legend, the reader is referred to the web version of this article.)

the objective to demonstrate the capacity of the compared image contrast enhancement techniques to extract information from an image, the averaged results in terms of the indexes Structural Similarity index measurement (*SSIM*), Mean squared error (*MSE*), Edge Preserve Index (*EPI*), Entropy (*E*), Relative Enhancement Contrast (*REC*) and Range Redistribution (*RR*) are registered in [Table 1](#) for all 116 images from the CSIQ dataset. High values denote a better performance for all metrics except for the *MSE*, which corresponds to the opposite effect. The *SSIM* and *EPI* indexes are two factors that indirectly assess the visual perception of an image. They evaluate the amount of edge information of the processed image. A higher value of *SSIM* represents an image that better preserves the important details. According to [Table 1](#), the *SSIM* and *EPI* metrics reveal with the highest values that the proposed MSA-ICE method presents the best performance in preserving the relevant edges and significant features present in the original image, making it suitable for feature related processing tasks. As can be seen from [Table 1](#), our proposed method obtains the lowest *MSE* elements. Low *MSE* values also determine a minimum distortion or error in the processed image. One of the best indexes that reflex the ability of a method to extract fine details from an image is the entropy (*E*). It quantitatively evaluates the information content present in an image. Results from [Table 1](#) demonstrates that the entropy (*E*) value from the proposed scheme is comparatively higher, which evaluates the quality of the enhanced image in terms of its information content.

With a high *REC* value, the proposed algorithm shows that it is able to produce images with significantly more contrast than its competitors. The value of the Range Redistribution (*RR*) is also a representative index to evaluate the capacity of an image contrast enhancement scheme to highlight hidden details. Under such conditions, an image with a high *RR* value means that more features can be detected and exhibited from the image. According to the *RR* index, it is clear that the proposed MSA-ICE presents the highest value. This means that the proposed algorithm provides the best pixel intensity redistribution without allowing their concentration. The remarkable performance of the proposed MSA-ICE is a result of the replacement of sporadic characteristics contained in the original image by meaningful pixel intensities contained in it.

After an analysis of [Table 1](#), it is observed that the proposed MSA-ICE scheme presents the best-averaged values among the considered algorithms. Its results have demonstrated that it reaches the best values with regard to the *SSIM*, *MSE*, *EPI*, *E*, *REC* and *RR* indexes. The approaches Fuzzy-IPSO, Gamma-PSO and ABC present the second place in terms of most of the performance indexes. The third category is represented by the CLAHE and WTHE techniques. Finally, the DE and FFA methods produce the worst results.

On the other hand, the averaged results of the eight algorithms considering all the 250 images from the TID2013 dataset, are

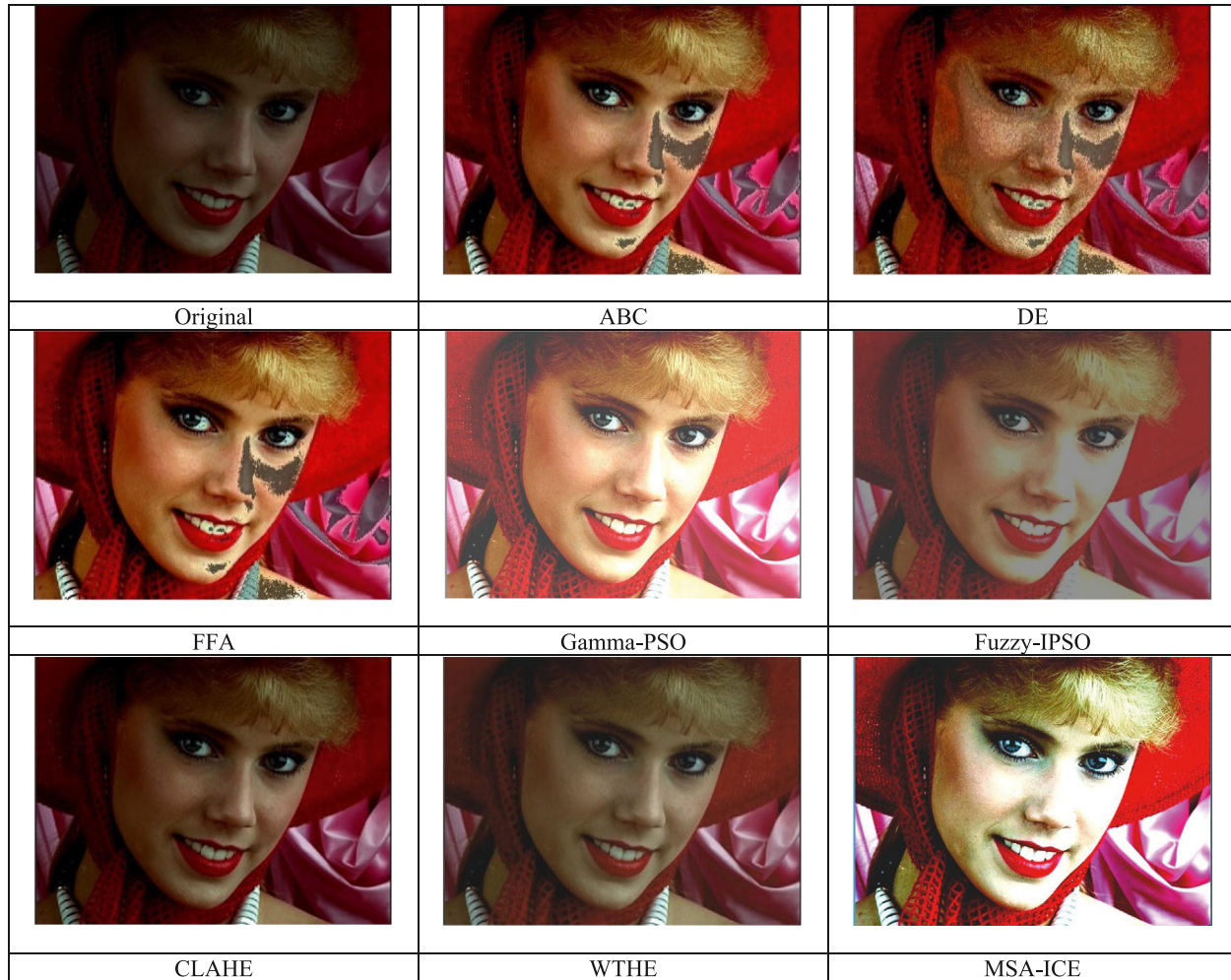


Fig. 16. Contrast enhancement results of the color image IC_5 for ABC, DE, FFA, Gamma-PSO, Fuzzy-IPSO, CLAHE, WTHE and MSA-ICE methods.. (For interpretation of the references to color in this figure legend, the reader is referred to the web version of this article.)

shown in [Table 2](#). The MSA-ICE attained the best performance indexes. Likewise, as the CSIQ dataset, the approaches Fuzzy-IPSO, Gamma-PSO and ABC present the second place in terms of most of the performance indexes while CLAHE and WTHE techniques reach the third category with performance slightly minor. On the other hand, the DE and FFA methods produce the worst results. The remarkable results of the proposed method are attributed to two important elements. One of them is the use of an elimination process. This mechanism allows deleting unimportant information for the enhancement process. As a consequence, it is possible to use the complete range of the histogram. This fact can be verified by the RR value, which implies that the proposed method reaches a better redistribution of the pixel intensities. The second factor is the use of the MSA algorithm. With the incorporation of MSA, the search strategy to obtain the best redistribution of the reduced histogram improves the exploration-exploitation capacities significantly. Therefore, the algorithm avoids being trapped in local minima. Under such conditions, the proposed method is able to obtain the best possible enhanced image in terms of the KL-entropy.

In order to analyze the quantitative and qualitative results in detail, a set of six representative images $I_1 - I_6$ have been selected from both dataset CSIQ and TID2013. The images are shown in [Figs. 5–10](#). All selected images are considered special cases due to their complexity.

[Table 3](#) presents the quantitative results among the algorithms for images $I_1 - I_6$. The Table reports the performance indexes in terms of Structural similarity index measurement ($SSIM$), Mean squared error (MSE), Edge Preserve Index (EPI), Entropy (E), Relative Enhancement Contrast (REC) and Range Redistribution (RR). From [Table 3](#), it is evident that the proposed MSA-ICE presents better performance index values than its competitors. In general, the methods DE and GSA exhibit a bad performance. This fact emphasizes that such methods need to be executed several times in order to produce consistent results. If they are evaluated only one time, the possibility to obtain a suboptimal solution is high. As a consequence of this problem, such algorithms produce frequently distorted images. In the case of the ABC, WTHE, CLAHE and FFA algorithms, they maintain a good performance in most of the performance indexes. However, as it can be seen in the RR index, they are not able to redistribute the intensities correctly in the enhanced result. This fact is evident from the visual perception of the produced images in comparison with the proposed MSA-ICE method.

Besides to the quantitative evaluation, a qualitative analysis is an important part to produce consistent conclusions when it is assessed the performance of contrast enhancement schemes. The objective of the qualitative analysis is to evaluate the presence of annoying distortions and other artifacts in the enhanced images attributed to a deficient operation of the used algorithms.

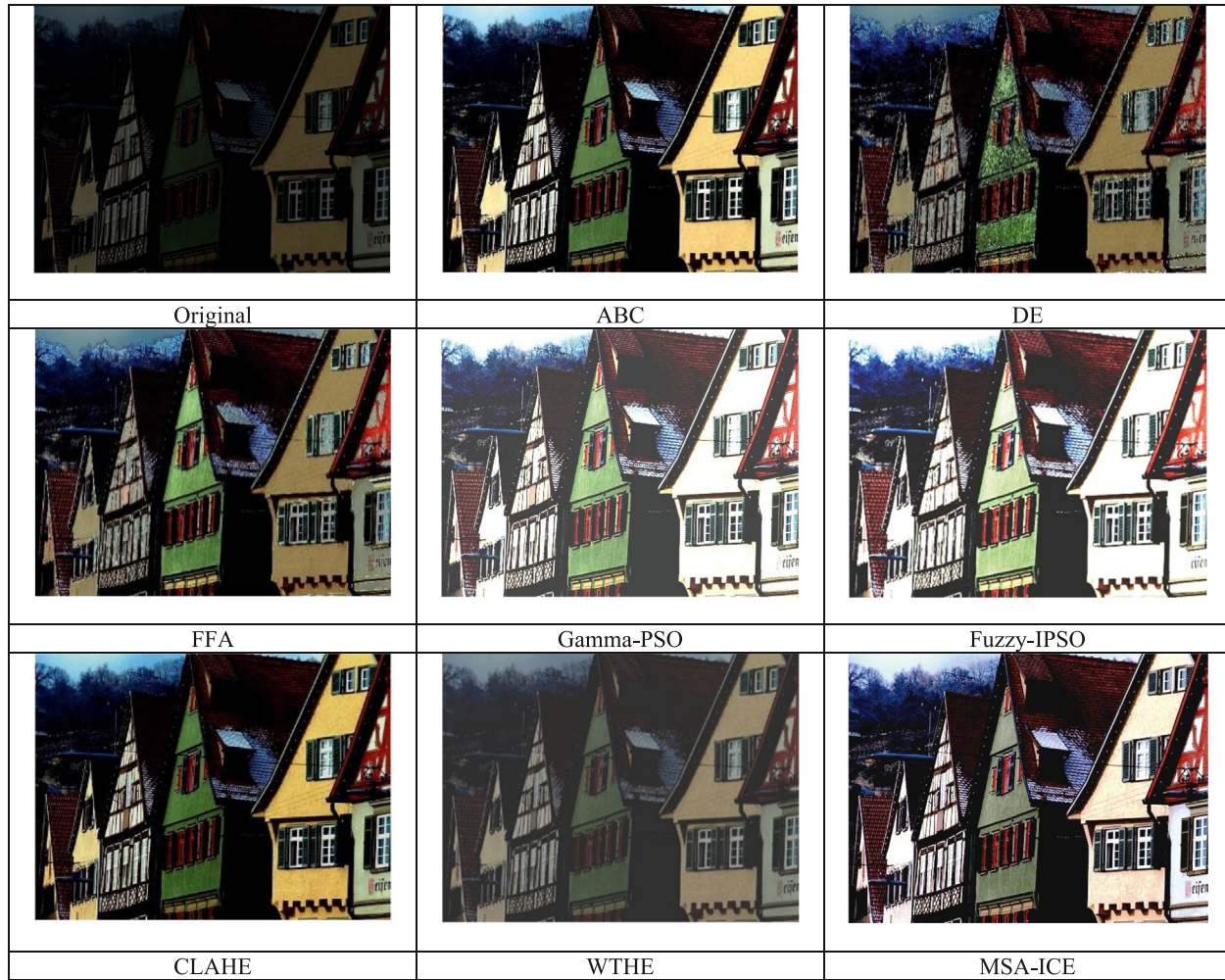


Fig. 17. Contrast enhancement results of the color image IC_6 for ABC, DE, FFA, Gamma-PSO, Fuzzy-IPSO, CLAHE, WTHe and MSA-ICE methods.. (For interpretation of the references to color in this figure legend, the reader is referred to the web version of this article.)

Each figure from 5 to 10 shows the original gray image along with contrast enhancement results obtained by the ABC, DE, FFA, Gamma-PSO, Fuzzy-IPSO, CLAHE, WTHe approaches and proposed MSA-ICE method. Analyzing the figures, in general, the Gamma-PSO and the Fuzzy-IPSO methods are able to efficiently enhance the contrast. However, their results present an excessive pixel modification. As a consequence, the pixel intensities are displaced to extremely bright and dark values. Moreover, ABC generates a bad enhancement effect since most of its images is not possible to differentiate important details. Results of DE and FFA methods introduce undesired artifacts. The quality of the images produced by these schemes also presents degradation. The scheme CLAHE produces images with darker intensities, which makes difficult to distinguish details and provides an unpleasant view. The WTHe approach maintains a slightly better image quality than CLAHE. Nevertheless, contrast-enhancement is unbalanced. Regions of the image present an appropriate contrast level while other regions still suffer the problem of intensity saturation. The enhanced images of Gamma-PSO and the Fuzzy-IPSO methods are significantly better than those produced by ABC, DE, FFA and CLAHE, but they also present difficulties with the intensity saturation. The results in the images of the Gamma-PSO and the Fuzzy-IPSO methods shows that they do not enhance the contrast appropriately. They generate enhanced images that are a little bit white or a little bit black, for the Gamma-PSO and the Fuzzy-IPSO, respectively. From Figs. 5–10, it can be observed that

the proposed MSA-ICE method presents in most of the images a better visual perception in comparison with its competitors (an exception is in Fig. 8). In the enhanced images by the MSA-ICE technique, details and important elements are clearly displayed, while the other algorithms maintain interesting hidden structures. This remarkable performance is a consequence of its robust mechanism to eliminate noise and very small structures that not present a visual effect. This extension makes the details in the image more distinguishable for human interpretation. A close inspection of the enhanced images indicates that the MSA-ICE technique presents a better pixel distribution (there is no saturation from white of dark regions) within the dynamic range when it is compared to the other methods. On the contrary, other ICE schemes produce several numbers of artifacts as a consequence of their improvement processes or generate a deficient distribution of pixel intensities.

In order to evaluate the computational cost CC, an experiment has been conducted. The study aims to measure the averaged computing time spent by the eight algorithms required to calculate an enhanced image (see Fig. I_1 – I_6). Table 4 shows the average times for every enhancement scheme. Each value is obtained as the averaged computational time after processing all six images from Figs. 5–10. From the Table, it is evident that the proposed MSA-ICE is the fastest method to obtain an enhancement image while the Gamma-PSO and Fuzzy-IPSO methods exhibit the highest computational cost (time elapsed). The main reason for the

Table 3

Image	Index	ABC	DE	FFA	Gamma-PSO	Fuzzy-IPSO	CLAHE	WTHE	MSA-ICE
I_1	SSIM	0.8745	0.6751	0.7574	0.8733	0.8824	0.7874	0.8014	0.9121
	MSE	7.32E+03	8.25E+03	8.12E+03	7.41E+03	7.35E+03	7.26E+03	7.26E+03	7.22E+03
	EPI	1.1974	0.9874	1.0074	1.1899	1.2008	1.0567	1.0987	1.3412
	E	6.1721	5.1047	5.8741	6.0987	6.1894	5.9740	6.0041	6.8714
	REC	1.1007	0.9421	0.9815	1.0965	1.1101	1.0010	1.0657	1.2101
	RR	43.1271	36.4197	39.4108	43.0014	44.2101	38.7410	41.7131	47.1240
I_2	SSIM	0.7422	0.6657	0.6871	0.7398	0.7592	0.7011	0.7127	0.7941
	MSE	5.02E+03	6.11E+03	5.87E+03	5.03E+03	4.98E+03	5.67E+03	5.41E+03	4.71E+03
	EPI	1.0041	0.8432	0.8741	1.0004	1.0940	0.9642	0.9857	1.0874
	E	5.5124	3.8297	4.1702	5.3897	5.6721	4.5787	4.8974	5.8471
	REC	0.9841	0.8714	0.8897	0.8897	0.9900	0.9057	0.9657	1.0074
	RR	36.4170	28.9840	30.7425	36.0120	37.5107	31.7421	33.8721	39.7487
I_3	SSIM	0.5621	0.4721	0.4897	0.5502	0.5800	0.5074	0.5214	0.60721
	MSE	3.69E+03	4.22E+03	4.10E+03	3.71E+03	3.68E+03	3.98E+03	3.87E+03	3.41E+03
	EPI	0.9721	0.8014	0.8971	0.9604	0.9740	0.9101	0.9510	0.9814
	E	4.4101	3.6512	3.7841	4.3821	4.5997	3.9740	4.0147	4.8721
	REC	0.9410	0.8011	0.8214	0.9304	0.9604	0.8714	0.8921	0.9941
	RR	39.1781	31.1487	33.1470	39.0011	40.0087	35.7840	37.8710	42.3180
I_4	SSIM	0.6321	0.5374	0.5847	0.62987	0.6501	0.6024	0.6121	0.6921
	MSE	6.18E+03	7.34E+03	6.68E+03	6.27E+03	6.25E+03	6.36E+03	6.24E+03	6.21E+03
	EPI	1.1014	0.9014	0.9874	1.0984	1.1001	1.0009	1.0874	1.2101
	E	4.8714	3.6874	3.8712	4.8004	4.9001	4.0874	4.2471	5.1401
	REC	1.0874	0.9514	0.9741	1.0074	1.0970	0.9872	1.0214	1.1921
	RR	31.0142	24.0142	26.1424	30.5784	32.0120	27.1024	29.4710	35.8724
I_5	SSIM	0.9611	0.8011	0.8724	0.9501	0.9604	0.9417	0.9510	0.9714
	MSE	7.31E+03	8.57E+03	8.25E+03	7.42E+03	7.10E+03	8.01E+03	7.81E+03	7.02E+03
	EPI	0.9841	0.8011	0.8741	0.9704	0.9004	0.9014	0.9410	1.0254
	E	6.1411	5.1472	5.5741	6.0874	6.1009	5.8914	6.0014	7.1101
	REC	0.9747	0.7547	0.8154	0.9667	0.9698	0.8874	0.9211	1.0074
	RR	35.1574	28.3210	30.4178	34.0098	34.9870	31.0440	33.1420	37.1421
I_6	SSIM	0.6187	0.4874	0.5017	0.6087	0.6211	0.5514	0.5784	0.6421
	MSE	3.43E+03	4.31E+03	4.10E+03	3.50E+03	3.40E+03	3.87E+03	3.58E+03	3.10E+03
	EPI	1.0874	0.8524	0.8974	0.9007	1.0047	0.9821	1.0044	1.1121
	E	5.0142	4.0020	4.4421	5.0071	5.0989	4.7784	4.8974	5.2140
	REC	1.0478	0.8745	0.90142	0.9870	0.9921	0.9974	1.0009	1.1987
	RR	43.2014	35.1470	37.2180	40.3710	43.3100	39.5870	41.0187	45.1470

Table 4

Averaged times for every enhancement scheme after processing images $I_1 - I_6$.

Algorithm	Execution time[s]
ABC	260.1478
DE	190.2410
FFA	204.2132
Gamma-PSO	340.6623
Fuzzy-IPSO	315.9021
CLAHE	169.4721
WTHE	158.2870
MSA-ICE	139.4101

Table 5

Performance comparison of the proposed objective function J_p with other objective functions J_1 and J_2 considering the 116 images from the CSIQ dataset.

Index	J_1	J_2	J_p
SSIM	0.4010	0.4521	0.8620
MSE	7.22E+03	6.41E+03	5.22E+03
EPI	0.9047	1.0991	1.2491
E	4.8874	5.4570	6.3871
REC	0.8514	0.9011	1.1272
RR	36.7814	39.2410	43.0121

excessive use of the computational time of the Gamma-PSO and Fuzzy-IPSO techniques is the significant number of computational phases in which they divide their contrast, improving processes. On the other hand, the ABC, DE and FFA present a moderated computational cost. These metaheuristic methods, according to the literature [23,24], require a higher number of iterations than

the MSA to obtain acceptable results. According to **Table 4**, although the CLAHE and the WTHE maintain a small computational overload, such values are superior to those produced by the proposed MSA-ICE method. Under these results, it is clear that the MSA-ICE presents the best performance in terms of SSIM, MSE, EPI, E, REC, RR and CC.

6.2. Comparison considering different objective functions

In this subsection, the enhancement contrast results produced by the proposed objective function J_p (Eq. (16)) based on the KL-entropy are compared to those produced by other objective functions used in the literature for contrast enhancement.

In the study, two representative objective functions have been considered. The first objective function J_1 proposed in [12] uses the number of edges and the Entropy to evaluate the quality of the enhanced image \mathbf{I} . This objective function is modeled as follows:

$$J_1 = \log \left(\sum_{i=0}^{L-1} P(q) \cdot \log (P(q)) \right) \cdot NE(\mathbf{I}) \quad (28)$$

where $P(q)$ refers to the probability density function at the intensity level q ($q \in 0, \dots, L-1$) of the image \mathbf{I} . L symbolizes the total number of grayscale levels represented in \mathbf{I} . $NE(\mathbf{I})$ represents the number of edge pixels present in \mathbf{I} computed through the use of the Sobel operator.

The second objective function J_2 proposed in [20] considers the combination of three different indexes such as Entropy (En), Contrast evaluation (CE) and the number of edges (NE). Therefore,

J_2 is formulated as follows:

$$J_2 = \sqrt{\frac{En + CE(\mathbf{I}) + NE(\mathbf{I})}{3}} \quad (29)$$

The Entropy (En) and Contrast evaluation (CE) are computed considering the following expressions:

$$En = \sum_{i=0}^{L-1} P(q) \cdot \log(P(q)) \quad CE(\mathbf{I}) = \frac{1}{M \times N} \sum_{i=1}^M \sum_{j=1}^N (\mathbf{I}(i, j) - \bar{I})^2 \quad (30)$$

where \bar{I} represents the intensity mean of the complete enhanced image \mathbf{I} .

In the experiment, the same metaheuristic algorithm MSA is used to find the best redistribution while a different objective function (J_1, J_2 and J_p) is employed to evaluate the solution quality. In the study, the results of the three different objective functions have been obtained from their operation of the complete number of images contained in the CSIQ dataset. In all experiments, the population size has been set to $N = 30$, while the maximum number of iterations is set to $k_{\max} = 100$. Such a stop criterion has been selected in order to keep compatibility with other similar works reported in the literature [39].

Table 5 shows the average values of each performance index over the set of 116 images from CSIQ. A close inspection of **Table 1** shows that the proposed objective function J_p presents the best-averaged values among the considered objective functions J_1 and J_2 . This fact means that J_p delivers not only the best possible data distribution in terms of the information contained but also the distribution with the best similitude concerning the original image data avoiding the distortion and artifacts. The second objective function J_2 presents the second place in terms of the performance indexes while the objective function J_1 produce the worst results. It is also remarkable that the proposed objective function J_p based on the KL-entropy obtains the best Range Redistribution (RR) index. This fact demonstrates that J_p allows a better redistribution of the information avoiding concentration of pixel intensities about J_1 and J_2 .

6.3. Comparison over grayscale images in terms of different metaheuristic techniques

Metaheuristic schemes, such as the MSA algorithm, are employed to obtain the solution of complex optimization problems. They are devised to be adequate for specific problems since no single metaheuristic method can solve all problems efficiently. Under such conditions, the performance of a metaheuristic scheme must be appropriately evaluated. Many comparisons among metaheuristic techniques have been published in the literature. However, they present an important limitation: their results are obtained over a set of synthetic functions with well-known behaviors and exact solutions, without considering their application scenario.

In this subsection, the performance of the MSA method is analyzed in terms of the contrast enhancement process, considering as objective function the Eq. (16) based on KL-entropy. Its results have been compared to those produced by the other metaheuristic optimization techniques such as the Artificial Bee Colony (ABC) algorithm [14], Differential Evolution (DE) [38], Gravitational Search Algorithm (GSA) [18] and Firefly Algorithm (FA) [17]. The specific parameter setup for the ABC, DE and FFA schemes is the same as that specified in Section 6.1. On the other hand, the GSA is configured as follows: The initial value for the gravitation constant is set to $G_0 = 100$, while the constant parameter alpha is set as $\alpha = 20$ [18].

In the experiments, the set of representative images I_1 – I_6 from **Figs. 5–10** have been considered. The objective of this experiment is to demonstrate that the MSA method presents a remarkable behavior to find the best redistribution in the enhancement process, avoiding being trapped in local optima. In the comparison, five different indicators are considered: The best solution f_{best} , the worst solution f_{worst} , the mean solution f_{mean} , the median solution f_{median} and the standard deviation f_{std} . Each contrast enhancement method is tested over every image by using 30 independent executions. As a consequence of this process, 30 different results of Fit (H_R) (Eq. (16)) are generated. Therefore, f_{best} represent the best-found solution from 30 values of Fit (H_R) while the worst value is identified as f_{worst} . The mean solution of these 30 outcomes is calculated to obtain f_{mean} . Likewise, the median values from these 30 results is calculated to obtain f_{median} . Finally, the standard deviation from the 30 results is computed to get the f_{std} solution. Indexes $f_{best}, f_{worst}, f_{mean}$ and f_{median} evaluate the approximation of the produced solutions while f_{std} the robustness of the contrast enhancement method.

The results, corresponding to 30 independent executions for each method, are reported in **Table 6**. The comparisons are analyzed by considering the performance indexes $f_{best}, f_{worst}, f_{mean}, f_{median}$ and f_{std} . Experimental evidence provided by **Table 6** demonstrates that the proposed MSA approach delivers significantly better results (maximal values) in comparison to those produced by the other methods. From the results, it is clear that the GSA scheme converges prematurely to a local maximum.

6.4. Comparison of color images

In this subsection, the performance of our proposed MSA-ICE method has been extended to consider color images. Its results are also compared with those produced by other schemes such as the Artificial Bee Colony (ABC) algorithm [14], Differential Evolution (DE) [38] and Firefly Algorithm (FFA) [17], the Gamma-PSO algorithm [20] and the Fuzzy-IPSO method [21], the Local and Adaptive Histogram Equalization (CLAHE) [8] and the Weighted thresholded Histogram Equalization (WTHE) [9].

Under the color enhancement scheme, firstly, an original input color image $I_{RGB} = \{RGB\}$ in Red, Green, and Blue (RGB) format is considered. Then, The I_{RGB} image is transformed into HSI space $I_{HSI} = T\{I_{RGB}\}$. From this I_{HSI} image, the intensity I -channel is processed for contrast enhancement as in the case of grayscale images. Finally, the enhanced I -channel along with the planes H and S are transformed back to the RGB space.

In order to evaluate the performance of each enhancement scheme over color images, the same six performance indexes used in the case of grayscale images have been considered in our analysis: Structural similarity index measurement (SSIM), Mean squared error (MSE), Edge Preserve Index (EPI), Entropy (E), Relative Enhancement Contrast (REC) and Range Redistribution (RR).

Additional to these indexes, it is also included the Colorfulness (C) index. The colorfulness (C) index [40] expresses the color contents in an image from a visual perspective. A higher value of C indicates a better color perception. Considering R, G and B as the color channels of an I_{RGB} image, C is computed as follows:

$$C = \sigma_{RGYB} + (0.3 \times \mu_{RGYB}) \quad (31)$$

where

$$\sigma_{RGYB} = \sqrt{\sigma_{RG}^2 + \sigma_{YB}^2} \quad \mu_{RGYB} = \sqrt{\mu_{RG}^2 + \mu_{YB}^2} \quad (32)$$

This metric evaluates the color perception as a function of the mean μ and standard deviation σ of all pixels contained in the

Table 6Performance results of ABC, DE, FA, GSA, MSA in terms of the objective function for each image from $I_1 - I_6$.

		ABC	DE	FA	MSA-ICE	GSA
I_1	f_{best}	8.3021E-05	-9.3946E-11	-83.3445799	239.768911	-27.5748866
	f_{worst}	1.7807E-05	-1.5681E-09	-157.605614	120.396818	-62.7913761
	f_{mean}	3.2351E-05	-2.5627E-10	-124.982729	156.979902	-46.9371447
	f_{median}	2.8065E-05	-1.5559E-10	-127.791923	153.180999	-47.6883123
	f_{std}	1.4815E-05	3.281E-10	18.003993	22.5155784	8.42339971
I_2	f_{best}	0.0040786	-7.7514E-11	-200.706366	304.79439	-39.0419775
	f_{worst}	7.5212E-05	-1.2561E-10	-273.437793	263.339792	-150.332676
	f_{mean}	0.00032857	-9.1745E-11	-242.402576	284.670928	-87.3715575
	f_{median}	0.0001596	-9.1515E-11	-237.01505	283.576551	-88.8296675
	f_{std}	0.00071902	1.1513E-11	22.9687993	10.7332911	26.5575174
I_3	f_{best}	0.0035828	-8.781E-11	-89.6788823	191.258436	-11.5687404
	f_{worst}	0.0001412	-1.9929E-10	-169.945826	174.287047	-83.5914617
	f_{mean}	0.00087394	-1.0814E-10	-123.078405	180.490427	-56.3344625
	f_{median}	0.00056547	-1.03E-10	-100.358516	180.417433	-69.0447586
	f_{std}	0.00093826	2.1262E-11	33.2097933	4.14439612	23.6166717
I_4	f_{best}	16.7490028	-8.919E-11	-17.0997514	33.9544188	-4.99519205
	f_{worst}	3.5058E-05	-1.2773E-10	-29.9979348	22.9055029	-10.6570464
	f_{mean}	0.74256915	-1.0718E-10	-25.6800729	29.6958407	-8.2317065
	f_{median}	8.6057E-05	-1.0506E-10	-25.7403874	30.1263737	-8.0785434
	f_{std}	3.18674734	9.5663E-12	3.50303534	2.72610241	1.49040519
I_5	f_{best}	0.71729222	-7.2286E-11	-0.63298755	0.91735293	-0.41317112
	f_{worst}	8.9332E-06	-1.0993E-10	-0.7232744	0.73117568	-0.50635223
	f_{mean}	0.33422472	-9.1787E-11	-0.65835117	0.79974294	-0.46670659
	f_{median}	0.55615539	-9.2211E-11	-0.65579256	0.79697052	-0.46752599
	f_{std}	0.32018918	8.4288E-12	0.0193367	0.03761757	0.02402692
I_6	f_{best}	0.61679468	-6.2086E-11	-0.60573131	0.79490854	-0.44279736
	f_{worst}	2.5523E-06	-9.4708E-11	-0.67033251	0.71277209	-0.5178735
	f_{mean}	0.13467604	-7.5153E-11	-0.6417174	0.75247277	-0.48489713
	f_{median}	1.2197E-05	-7.4366E-11	-0.64253346	0.75207066	-0.48364784
	f_{std}	0.24874496	6.589E-12	0.01479577	0.02204985	0.01842073

channel differences RG and YB defined as follows:

$$RG = (R - G) \quad YB = 0.5 \times (G + B) - B \quad (33)$$

In the experiments, several color images extracted from the CSIQ and TID2013 databases have been used. However, for the sake of space, a set of three representative images have been considered. They are exhibited in Fig. 11. The images represent different complexities. The first three images (IC_1 , IC_2 and IC_3) exhibit images with a high color contain while the last three (IC_4 , IC_5 and IC_6) present low-light properties.

The results in terms of the indexes Structural similarity index measurement (SSIM), Mean squared error (MSE), Edge Preserve Index (EPI), Entropy (E), Relative Enhancement Contrast (REC), Range Redistribution (RR), and colorfulness (C) are registered in Table 4 for every image from Fig. 11. According to Table 7, the proposed method obtains the best performance indexes among all existing methods. While comparing the other existing techniques, the E value of the proposed method presents the highest value. Hence the original information content is maintained more. Results from Table 7 demonstrates that the RR values from the proposed scheme are comparatively higher, which evaluates the redistribution of the enhanced image. The proposed method of MSA-ICE produces the highest C values measure. Under such conditions, the proposed algorithm obtains more natural color content in comparison with the original input image. Therefore, the enhanced images also show adequate performance for human visualization. After an analysis of Table 7, it is demonstrated that our MSA-ICE method exhibits the best-averaged values among the considered algorithms in terms of the performance indexes. The approaches Fuzzy-IPSO, Gamma-PSO and ABC present the second place in terms of most of the performance indexes. The third category is represented by the CLAHE and WTHe techniques. Finally, the DE and FFA methods produce the worst results.

The visual results of the eight contrast enhancement methods are depicted in Figs. 12–17. Analyzing qualitatively, the figures,

in general, the ABC, DE and FFA methods, are able to enhance the images slightly. This poor enhancement is perceived through a loss of fine details in the images. These methods also produce different artifacts as a consequence of an abnormal increase and intensity saturation. This fact is attributed to the incapacity of such methods to operate with the objective function Eq. (16) and all its constraints. Under the complexity of this formulation, ABC, DE and FFA techniques identify only a sub-optimal solution (local solution) instead of the global solution. From the visual results, it can be seen that such solutions allow producing images with a mean brightness without considering the detail preservation. The study of visual observations demonstrates that the Gamma-PSO, Fuzzy-IPSO, CLAHE and WTHe approaches produce a relative success with regard to the contrast enhancement. Nevertheless, the images present an over-brightened or an over-darkened effect. The Gamma-PSO and CLAHE present a tendency to generate over-darkened results while Fuzzy-IPSO and WTHe produce over-darkened effect. These undesired effects avoid the observation of important details. Another problem associated with the over-brightened and over-darkened responses is the lack of perception of color. From the visual inspection, it is clear that the proposed MSA-ICE presents the best visual results. The proposed technique is able to produce images where details and important characteristics are highlighted. The approach allows modifying the pixel intensities in such a way that undesired effects are eliminated. In general, all approaches ABC, DE, FFA, Gamma-PSO, Fuzzy-IPSO, CLAHE, WTHe and the proposed MSA-ICE present a color distortion in most of the enhanced images. However, the MSA-ICE is the technique that produces the lower color distortion. The example of Fig. 13 presents the image with the highest magnitude of color distortion produced by the MSA-ICE method as it can be seen, such an image presents a distortion, although the other methods also exhibit a considerable color modification when it is compared with the MSA-ICE algorithm. The last three images

Table 7

Performance results of ABC, DE, FFA, Gamma-PSO, Fuzzy-IPSO CLAHE, WTHe and MSA-ICE in terms of the indexes (SSIM), Mean squared error (MSE), Edge Preserve Index (EPI), Entropy (E), Relative Enhancement Contrast (REC), Range Redistribution (RR) and colorfulness (C) for each image from Fig. 11.

Image	Index	ABC	DE	FFA	Gamma-PSO	Fuzzy-IPSO	CLAHE	WTHe	MSA-ICE
IC ₁	SSIM	0.8014	0.6574	0.7487	0.7921	0.8110	0.7651	0.7821	0.8854
	MSE	8.24E+03	9.34E+03	9.10E+03	8.34E+03	8.15E+03	8.87E+03	8.65E+03	8.01E+03
	EPI	1.0121	0.9012	0.9651	0.9032	0.9891	0.9874	1.091	1.1247
	E	6.1041	4.9870	5.1274	5.8341	6.1421	5.7428	5.8797	6.7421
	REC	1.0241	0.9754	1.0004	0.9841	0.9951	1.0094	1.0100	1.1241
	RR	42.8710	34.7481	36.4107	40.2251	42.7840	38.2170	40.8941	44.2781
IC ₂	C	0.31014	0.2574	0.2841	0.3006	0.2981	0.2978	0.3041	0.3341
	SSIM	0.6014	0.5412	0.5621	0.5902	0.5891	0.5832	0.5900	0.7021
	MSE	6.34E+03	7.02E+03	6.88E+03	6.50E+03	6.82E+03	6.75E+03	6.46E+03	6.17E+03
	EPI	0.9621	0.8210	0.8411	0.9231	0.8892	0.8941	0.9241	0.9874
	E	4.1074	3.2740	3.4174	3.8562	3.7831	3.7024	3.9875	4.8821
	REC	0.9014	0.8289	0.8421	0.8841	0.7961	0.8741	0.8832	0.9441
IC ₃	RR	36.2701	28.2278	30.7704	32.7241	30.7231	32.0147	34.2839	38.1420
	C	0.2874	0.2141	0.2214	0.2522	0.2401	0.2417	0.26471	0.3011
	SSIM	0.7512	0.6697	0.6874	0.7681	0.7751	0.7104	0.7247	0.8421
	MSE	7.57E+03	8.21E+03	8.07E+03	7.41E+03	7.38E+03	7.93E+03	7.81E+03	7.32E+03
	EPI	0.9074	0.7924	0.8154	0.9142	0.9201	0.8621	0.8874	0.9421
	E	3.8721	2.6270	2.8974	3.8803	3.9002	3.1421	3.6421	4.1014
IC ₄	REC	0.8040	0.7454	0.7528	0.8124	0.8241	0.7721	0.7974	0.8941
	RR	34.2210	27.2170	28.2247	34.2341	34.4581	30.8740	32.8740	36.2140
	C	0.2741	0.1987	0.2274	0.2781	0.2790	0.2422	0.2574	0.2987
	SSIM	0.7231	0.6532	0.6482	0.7421	0.7632	0.6931	0.7020	0.8021
	MSE	8.65E+03	9.11E+03	9.20E+03	8.54E+03	8.23E+03	8.84E+03	8.81E+03	7.89E+03
	EPI	0.8843	0.8042	0.8162	0.9321	0.9362	0.8654	0.8670	0.9765
IC ₅	E	3.9821	3.5672	3.6640	4.1023	4.2103	3.7892	3.8124	4.5672
	REC	0.8450	0.7853	0.8004	0.8572	0.8631	0.8021	0.8164	0.9023
	RR	33.0051	28.7489	29.8743	33.4561	35.5630	30.2385	32.6739	37.9632
	C	0.2084	0.1672	0.1899	0.2234	0.2373	0.1892	0.1903	0.2893
	SSIM	0.8842	0.7892	0.7994	0.8856	0.8870	0.8009	0.8182	0.9061
	MSE	7.93E+03	8.45E+03	8.37E+03	7.86E+03	7.80E+03	8.20E+03	8.18E+03	7.53E+03
IC ₆	EPI	0.9320	0.8563	0.8753	0.9662	0.9872	0.9032	0.9125	1.1261
	E	4.4676	4.0021	4.1292	4.6673	4.7032	4.2193	4.3389	5.9632
	REC	0.9537	0.8283	0.8772	0.9732	0.9862	0.9123	0.9245	1.2809
	RR	30.9850	22.7893	25.8303	31.6743	34.7620	27.8692	29.7630	38.9032
	C	0.2345	0.1782	0.2893	0.2253	0.2567	0.1945	0.2008	0.3892
	SSIM	0.8302	0.7984	0.8032	0.8573	0.8730	0.8122	0.8237	0.9032
IC ₇	MSE	8.22E+03	8.88E+03	9.00E+03	7.90E+03	8.03E+03	8.58E+03	8.40E+03	7.81E+03
	EPI	0.9243	0.8245	0.8641	0.9421	0.9643	0.8840	0.9003	0.9902
	E	4.1032	3.0037	3.2743	4.4052	4.7004	3.6783	3.8830	5.0393
	REC	0.9435	0.8673	0.8870	0.9356	0.9560	0.9054	0.9180	1.0342
	RR	32.6703	25.9730	28.9803	33.6704	35.9982	29.9045	30.9850	39.8701
	C	0.2560	0.1905	0.2076	0.2483	0.2589	0.2076	0.2167	0.3678

represent an interesting challenge since they correspond to images captured in low-light conditions. Under such circumstances, most of the ICE methods present a bad performance. This fact is a consequence of the big changes in intensity values that is necessary to carry out. Therefore, there exists a strong trend to generate intensity saturation and noise amplification in the enhanced image. Despite such conditions, the proposed MSA-ICE method presents the best performance in comparison with its competitors.

7. Conclusion

The existence of noise and small sets of pixel intensities affect the process of image enhancement negatively. Such elements correspond to sets of pixels that are too small to represent objects or visible details in the image. The presence of such elements does not allow the adjustment of the original image distribution in the complete range. In this paper, an Image Contrast Enhancement (ICE) algorithm for images is introduced. Our scheme divides the image contrast enhancement process into two steps: the elimination of irrelevant information and contrast improvement. In the first step, the Mean-shift method is employed to delete unimportant small sets of pixels. The objective is to replace these

sporadic characteristics contained in the original histogram by meaningful pixel densities represented by their local maxima. In the second step, the contrast of the reduced histogram is adjusted. For this propose, the Moth Swarm Algorithm (MSA) is used. Therefore, the Moth Swarm Algorithm (MSA) is adopted to redistribute the pixel intensities of the reduced histogram so that the value of the Kullback–Leibler Entropy (KL-entropy) between a candidate distribution and other considered as the best possible configuration has been maximized.

The performance of the proposed approach has been tested considering a representative set of different grayscale and color images commonly found in the literature. Its results are also compared with those produced by other similar techniques, such as artificial bee colony (ABC), differential evolution (DE), firefly algorithm (FFA), the Gamma-PSO algorithm, the Fuzzy-IPSO method, Local and Adaptive Histogram Equalization (CLAHE) and the Weighted thresholded Histogram Equalization (WTHe). Experimental results suggest that the proposed method has a better performance in comparison with other schemes in terms of different performance indexes that evaluate the enhancement quality.

As future work is planned to prove the algorithm using distinct contrast metrics as well as make a comparison between them.

Other ideas lead to finding modifications to improve the MSA algorithm with the aim to get better results and to apply the ICE to areas of interest as medical images, satellite images, among others.

CRediT authorship contribution statement

Alberto Luque-Chang: Conceptualization, Investigation, Methodology, Writing part of the document. **Erik Cuevas:** Project administration, Supervision, Validation, Writing - review & editing. **Marco Pérez-Cisneros:** Validation, Funding acquisition, Resources for the manuscript. **Fernando Fausto:** Formal analysis, Validation, Visualization, Writing of the manuscript. **Arturo Valdivia-González:** Software, Methodology. **Ram Sarkar:** Data curation, Formal analysis of the experimental results.

Declaration of competing interest

The authors declare that they have no known competing financial interests or personal relationships that could have appeared to influence the work reported in this paper.

References

- [1] Reid Smith, Knowledge-Based Systems Concepts, Techniques, Examples, Schlumberger-Doll Research, 2013.
- [2] M. Agarwal, R. Mahajan, Medical images contrast enhancement using quad weighted histogram equalization with adaptive gama correction and homomorphic filtering, *Procedia Comput. Sci.* 115 (2017) 509–517.
- [3] M. Agarwal, R. Mahajan, Medical image contrast enhancement using range limited weighted histogram equalization, *Procedia Comput. Sci.* 125 (2018) 149–156, <http://dx.doi.org/10.1016/j.procs.2017.12.021>.
- [4] J. Lewin, Comparison of contrast-enhanced mammography and contrast-enhanced breast MR imaging, *Magn. Reson. Imaging Clin. North Am.* 26 (2) (2018) 259–263, <http://dx.doi.org/10.1016/j.mric.2017.12.005>.
- [5] Sonali, S. Sahu, A.K. Singh, S.P. Ghlera, M. Elhoseny, An approach for denoising and contrast enhancement of retinal fundus image using CLAHE, *Opt. Laser Technol.* (2018) <http://dx.doi.org/10.1016/j.optlastec.2018.06.061>.
- [6] H.-T. Wu, S. Tang, J. Huang, Y.-Q. Shi, A novel reversible data hiding method with image contrast enhancement, *Signal Process., Image Commun.* 62 (2018) 64–73, <http://dx.doi.org/10.1016/j.image.2017.12.006>.
- [7] X. Wang, L. Chen, An effective histogram modification scheme for image contrast enhancement, *Signal Process., Image Commun.* 58 (2017) 187–198, <http://dx.doi.org/10.1016/j.image.2017.07.009>.
- [8] A.M. Reza, Realization of the contrast limited adaptive histogram equalization (clae) for real-time image enhancement, *J. VLSI Signal Process. Syst. Signal Image Video Technol.* 38 (2004) 35–44.
- [9] Q. Wang, R.K. Tan, Fast image/video contrast enhancement based on weighted thresholded histogram equalization, *IEEE Trans. Consum. Electron.* 53 (2) (2007) 757–764.
- [10] K. Manpreet, K. Jasdeep, K. Jappreet, Survey of contrast enhancement techniques based on histogram equalization, *Int. J. Adv. Comput. Sci. Appl.* 2 (7) (2015) 2011137.
- [11] E. Cuevas, M. Cienfuegos, A new algorithm inspired in the behavior of the social-spider for constrained optimization, *Expert Syst. Appl.* 41 (2) (2014) 412–425, <http://dx.doi.org/10.1016/j.eswa.2013.07.067>.
- [12] S. Hashemi, S. Kiani, N. Noroozi, M.E. Moghaddam, An image contrast enhancement method based on genetic algorithm, *Pattern Recognit. Lett.* 31 (13) (2010) 1816–1824, <http://dx.doi.org/10.1016/j.patrec.2009.12.006>.
- [13] L. Maurya, P.K. Mahapatra, A. Kumar, A social spider optimized image fusion approach for contrast enhancement and brightness preservation, *Appl. Soft Comput. J.* 52 (2017) 575–592, <http://dx.doi.org/10.1016/j.asoc.2016.10.012>.
- [14] D. Karaboga, B. Basturk, A powerful and efficient algorithm for numerical function optimization: Artificial bee colony (ABC) algorithm, *J. Global Optim.* 39 (3) (2007) 459–471, <http://dx.doi.org/10.1007/s10898-007-9149-x>.
- [15] J. Kennedy, R. Eberhart, Particle swarm optimization, in: *Neural Networks, 1995. Proceedings. IEEE International Conference On*, Vol. 4, 1995, pp. 1942–1948, <http://dx.doi.org/10.1109/ICNN.1995.488968>.
- [16] A.K. Bhandari, V. Soni, A. Kumar, G.K. Singh, Cuckoo search algorithm based satellite image contrast and brightness enhancement using DWT-SVD, *ISA Trans.* 53 (4) (2014) 1286–1296.
- [17] X.-S. Yang, Firefly algorithm, Lévy flights and global optimization, in: *Research and Development in Intelligent Systems XXVI*, 2010, pp. 209–218, http://dx.doi.org/10.1007/978-1-84882-983-1_15.
- [18] E. Rashedi, H. Nezamabadi-pour, S. Saryazdi, GSA: A gravitational search algorithm, *Inform. Sci.* 179 (13) (2009) 2232–2248, <http://dx.doi.org/10.1016/j.ins.2009.03.004>.
- [19] L. dos S. Coelho, J.G. Sauer, M. Rudek, Differential evolution optimization combined with chaotic sequences for image contrast enhancement, *Chaos Solitons Fractals* 42 (1) (2009) 522–529, <http://dx.doi.org/10.1016/j.chaos.2009.01.012>.
- [20] A. Mahmood, S. Khan, S. Hussain, E. Almaghayreh, An adaptive image contrast enhancement technique for low-contrast images, *IEEE Access* 7 (2019) 161584–161592.
- [21] B. Subrahmanyaswara-Rao, Dynamic histogram equalization for contrast enhancement for digital images, *Appl. Soft Comput. J.* 89 (2020) 106114.
- [22] A.-A.A. Mohamed, Y.S. Mohamed, A.A.M. El-Gaafary, A.M. Hemeida, Optimal power flow using moth swarm algorithm, *Electr. Power Syst. Res.* 142 (2017) 190–206, <http://dx.doi.org/10.1016/j.epsr.2016.09.025>.
- [23] Ashish Kumar Bhandari, K. Rahul, A context sensitive masi entropy for multilevel image segmentation using moth swarm algorithm, *Infrared Phys. Technol.* 98 (2019) 132–154, <http://dx.doi.org/10.1016/j.infrared.2019.03.010>.
- [24] M.A. Ibrahim, M. Becherif, A.Y. Abdelaziz, Dynamic performance enhancement for wind energy conversion system using Moth-Flame Optimization based blade pitch controller, *Sustain. Energy Technol. Assess.* 27 (2018) 206–212, <http://dx.doi.org/10.1016/j.seta.2018.04.012>.
- [25] Y. Aliyari Ghassabeh, F. Rudzicz, The mean shift algorithm and its relation to kernel regression, *Inform. Sci.* 348 (2016) 198–208, <http://dx.doi.org/10.1016/j.ins.2016.02.020>.
- [26] K.-L. Wu, M.-S. Yang, Mean shift-based clustering, *Pattern Recognit.* 40 (11) (2007) 3035–3052, <http://dx.doi.org/10.1016/j.patcog.2007.02.006>.
- [27] S. Kullback, R.A. Leibler, On information and sufficiency, *Ann. Math. Stat.* 22 (1) (1951) 79–86, <http://dx.doi.org/10.1214/aoms/1177729694>. JSTOR2236703.
- [28] B.C. Cabella, M.J. Sturzbecher, D.B. De Araujo, U.P. Neves, Generalized relative entropy in functional magnetic resonance imaging, *Phys. A* 388 (1) (2009) 41–50.
- [29] I. Horová, J. Koláček, J. Zelinka, Kernel smoothing in matlab, 2012, <http://dx.doi.org/10.1142/8468>.
- [30] M. Jamil, H.J. Zepernick, Lévy flights and global optimization, *Swarm Intell. Bio-Inspired Comput.* (2013) 49–72, <http://dx.doi.org/10.1016/B978-0-12-405163-8.00003-X>.
- [31] R.N. Mantegna, Fast, accurate algorithm for numerical simulation of Lévy stable stochastic processes, *Phys. Rev. E* 49 (5) (1994) 4677–4683, <http://dx.doi.org/10.1103/PhysRevE.49.4677>.
- [32] E.C. Larson, D.M. Chandler, Most apparent distortion: Full-reference image quality assessment and the role of strategy, *J. Electron. Imaging* 19 (1) (2010) 11006–11021.
- [33] N. Ponomarenko, L. Jin, O. Ieremeiev, V. Lukin, K. Egiazarian, J. Astola, B. Vozel, K. Chehdi, M. Carli, F. Battisti, C.C. Kuo, Image database TID2013: Peculiarities, results and perspectives, *Signal Process., Image Commun.* 30 (2015) 57–77.
- [34] J. Joseph, R. Periyasamy, A fully customized enhancement scheme for controlling brightness error and contrast in magnetic resonance images, *Biomed. Signal Process. Control.* 39 (2018) 271–283.
- [35] R. Nie, M. He, J. Cao, D. Zhou, Z. Liang, Pulse coupled neural network based MRI image enhancement using classical visual receptive field for smarter mobile healthcare, *J. Ambient Intell. Humaniz. Comput.* 10 (2019) 4059–4070.
- [36] C. Zhao, Z. Wang, H. Li, X. Wu, S. Qiao, J. Sun, A new approach for medical image enhancement based on luminance-level modulation and gradient modulation, *Biomed. Signal Process. Control.* 48 (2019) 189–196.
- [37] Z. Chen, B.R. Abidi, D.L. Page, M.A. Abidi, Gray-level grouping (GLG): An automatic method for optimized image contrast Enhancement—Part I: The basic method, *IEEE Trans. Image Process.* 15 (8) (2006) 2290–2302.
- [38] A.K. Qin, V.L. Huang, P.N. Suganthan, Differential evolution algorithm with strategy adaptation for global numerical optimization, *IEEE Trans. Evol. Comput.* 13 (2) (2009) 398–417, <http://dx.doi.org/10.1109/TEVC.2008.927706>.
- [39] K. Jayanthi, L.R. Sudha, Optimal gray level mapping for satellite image contrast enhancement using grey wolf optimization algorithm, *Int. J. Eng. Sci. Invent.* 45 (2018) 38–44.
- [40] S.E. Suesstrunk Hasler, Measuring colorfulness in natural images, *Electronic Imaging, Int. Soc. Opt. Photon.* (2003) 87–95.G.